공학박사 학위논문

MAC Layer Strategies for Cellular Sidelink Performance Enhancements

셀룰러 사이드링크 성능 향상을 위한 상위계층 기법

2020년 8월

서울대학교 대학원

전기·정보 공학부

윤 호 영

MAC Layer Strategies for Cellular Sidelink Performance Enhancements

지도 교수 박 세 웅

이 논문을 공학박사 학위논문으로 제출함

2020년 7월

서울대학교 대학원

전기·정보공학부

윤 호 영

윤호영의 공학박사 학위 논문을 인준함

2020년 6월

위 원 장:	심 병 효	(인)
부위원장:	박 세 웅	(인)
위 원:	오 정 석	(인)
위 원:	이 경 한	(인)
위 원:	백 정 엽	(인)

Abstract

In typical cellular communications, User Equipments (UEs) have always had to go through a Base Station (BS) to communicate with each other, e.g., a UE transmits a packet to a BS via uplink and then the BS transmits the packet to another UE via downlink. Although the communication method can serve UEs efficiently, the communication method can cause latency problems and overload problems in BS. Thus, sidelink has been proposed to overcome these problems in 3GPP release 12. Through sidelink, UEs can communicate directly with each other.

There are two representative communications using sidelink, i.e., Device-to-Device (D2D) communication and Vehicle-to-Vehicle (V2V) communication. In this dissertation, we consider three strategies to enhance the performances of D2D and V2V communications: (i) efficient feedback mechanism for D2D communications, (ii) context-aware congestion control scheme for V2V communication, and (iii) In-Device Coexistence (IDC)-aware LTE and NR sidelink resource allocation scheme.

Firstly, in the related standard, there is no feedback mechanism for D2D communication because D2D communications only support broadcast-type communications. A feedback mechanism is presented for D2D communications. Through our proposed mechanism, UEs can use the feedback mechanism without the help of BS and UEs do not need additional signals to allocate feedback resources. We also propose a rate adaptation algorithm, which consider in-band emission problem, on top of the proposed feedback mechanism. We find that our rate adaptation achieves higher and stable throughput compared with the legacy scheme that complies to the standard.

Secondly, we propose a context-aware congestion control scheme for LTE-V2V communication. Through LTE-V2V communication, UEs transmit Cooperative Awareness Message (CAM), which is a periodic message, and Decentralized Environmental Notification Message (DENM), which is a event-driven message and allows one-hop relay. The above two messages have different characteristics and generation rule. Thus, it is difficult and inefficient to apply the same congestion control scheme to two messages. We propose a congestion control schemes for each message. Through the proposed congestion control schemes, UEs decide whether to transmit according to their situation. Through simulation results, we show that our proposed schemes outperform comparison schemes as well as the legacy scheme.

Finally, we propose a NR sidelink resource allocation scheme based on multi-agent reinforcement learning, which awares a IDC problem between LTE and NR in Intelligent Transport System (ITS) band. First, we model a realistic IDC interference based on spectrum emission mask specified at the standard. Then, we formulate the resource allocation as a multi-agent reinforcement learning with fingerprint method. Each UE achieves its local observation and rewards, and learns its policy to increase its rewards through updating Q-network. Through simulation results, we observe that the proposed resource allocation scheme further improves Packet Delivery Ratio (PDR) performances compared to the legacy scheme.

keywords: LTE, NR, device-to-device communications, vehicle-to-vehicle communications, feedback mechanism, congestion control, in-device coexistence, reinforcement learning.

student number: 2014-21660

Contents

List of Tables

List of Figures

Chapter 1

Introduction

1.1 Motivation

In typical cellular communications, User Equipments (UEs) have always had to go through a Base Station (BS) to communicate with each other, e.g., a UE transmits a packet to a BS via uplink and then the BS transmits the packet to another UE via downlink. Although the communication method can serve UEs efficiently, the communication method can cause latency problems and overload problems in BS. Thus, sidelink has been proposed to overcome these problems in 3GPP release 12. Through sidelink, UEs can communicate directly with each other.

There are two representative communications using sidelink, i.e., Device-to-Device (D2D) communication and Vehicle-to-Vehicle (V2V) communication. In this thesis, we focus on enhancements of sidelink performances. In case of D2D communication, there is no feedback mechanism for D2D communication because D2D communication only support broadcast-type communications. Therefore, in D2D scenario, transmitters (TXs) transmit their packets inefficiently. We propose a feedback mechanism to transmit feedback so that the TXs can effectively transmit packets.

In case of V2V communications, we focus on two problems. The first problem is a radio resource congestion problem. There are two reasons why the congestion problem occurs frequently. Firstly, there is a scarcity of wireless bandwidth in LTE-V2V. Intelligent Transport System (ITS) band, which is a 5.9 GHz band, is dedicated to vehicular communications. Most countries consider allocating two channels for LTE-V2V. Considering not only V2V but also Vehicle-to-Infrastructure (V2I) operations over the two allocated channels, the bandwidth is not enough. Secondly, different from Cooperative Awarness Message (CAM) traffic, which does not take into account relay operation, Decentralized Environmental Notification Message (DENM) traffic allows one-hop relay. Therefore, the radio resource congestion problem can be more severe due to DENM relaying at receivers. In addition, multiple source UEs can be generated for a single event, i.e., it is possible that multiple source UEs generate redundant DENMs and cause congestion problems.

The second problem is a In-Device Coexistence (IDC) problem between LTE and NR sidelinks. The current smartphones are equipped with two or more RF modules. When these RF modules operate simultaneously at adjacent channels, they interfere with each other by Out-of Band (OOB) emission. This problem is called an IDC problem. Since NR does not support backward compatibility with LTE, LTE and NR installed as independent RF modules in a device. In the related standard, NR sidelink can also operate at ITS band. As a result, IDC problem between LTE and NR can also occur.

1.2 Overview of Existing Approaches

1.2.1 Efficient feedback mechanism for LTE-D2D communication

There are many studies [1–9], which support feedback mechanism as part of D2D communications. However, in most studies [1–7], the authors assume the situation where BS receives feedback from D2D UEs while we support a feedback mechanism between D2D Tx and D2D Rxs. Moreover, in most studies [1–8], it is assumed that cellular and D2D UEs share the same resource pool for data transmission and unicast scenarios are considered. In contrast, in our work, D2D UEs do not share the resource pool with cellular UEs as defined in 3GPP LTE-based D2D communication and we also consider groupcast scenarios. Zhou *et al.* [9] consider groupcast, but they assume that D2D Txs perfectly acquire data receiving result of all D2D Rxs belonging to the same group. However, they do not provide any clear methodology of a feedback mechanism, thus making the work impractical.

1.2.2 CoCo: Context aware congestion control scheme for C-V2X communications

There are several related studies. To the best of our knowledge, there are very few congestion control schemes for C-V2V. However, there are related studies for Dedicated Short Range Communication (DSRC) which is IEEE 802.11p based vehicular communication. Therefore, we conducted more research on DSRC studies to learn trends in congestion control schemes and to find appropriate comparison schemes.

As far as we have surveyed, relevant studies mainly depend on channel load measurements or Channel Busy Ratio (CBR) [10–20]. They adjust transmission parameters such as transmission interval, transmission power, and data rate, based on channel load measurements (or CBR). For example, if the channel load is greater than a pre-defined threshold, the UE increases its transmission interval to reduce the channel load.

However, since channel load measurements fluctuate very much, channel load measurement based solutions are not reliable. In vehicular communication environments, channel load fluctuations become greater with higher mobility. To show how the channel measurement is affected by high mobility, we measure real Received Signal Strength (RSS) samples by comparing the cases with and without mobility. We present the details about the result of the channel measurement in Section 3.2.1.

There are other studies [21–23], which use context information such as UE's location and speed. The study in [21] is application-limited, i.e., lane change. In this study, when the UE attempts to change a lane, it reduces transmission power since it should only communicate with the UEs closest to the UE behind. This study does not apply to controlling the transmission parameters of CAM or DENM, which must be shared with all neighboring UEs. The authors in [22, 23] use context for mitigating the congestion problem.

1.2.3 IDC-aware resource allocation based on multi-agents reinforcement learning

Since NR standalone V2V has not been completed, there are no studies dealing with IDC problem between NR and LTE sidelinks. However, there are some studies considering IDC problem between LTE and WLAN [24–26]. There is also a study considering IDC problem between LTE and GNSS [27]. However, All of the above authors consider the resource allocation method of the base station.

We also surveyed multi-agent reinforcement learning-based resource allocation for V2V communication. There are several studies [28–30]. In [28, 29], the authors consider that UEs select resources via multi-agent reinforcement learning. However, they do not consider IDC problem, i.e, they only take into account the interference generated by the same resource selection.

1.3 Main Contributions

1.3.1 Efficient feedback mechanism for LTE-D2D communication

We propose a feedback mechanism for D2D communication to complement the absence of feedback mechanism. We also propose a groupcast rate adaptation algorithm, which is FaRRA, considering in-band emission problem.

Two key contributions of this chapter can be summarized as follows.

- This is the first time a feedback mechanism for LTE-based D2D Tx and Rxs has been proposed, to our best knowledge.

- The proposed feedback mechanism does not require additional signaling for feedback scheduling and allows multiple D2D Rxs to use the same radio resource to improve spectral efficiency.

- We also propose a feedback-based rate adaptation and retransmission schemes for D2D groupcast communication and verify that the proposed solutions achieve solid performance, e.g., goodput, in various channel environments.

With these contributions, receivers (RXs) can use feedback for the enhancements of their performances by using small resources

1.3.2 CoCo: Context aware congestion control scheme for C-V2X communications

We propose a context aware congestion control scheme for C-V2X communication, called CoCo. CoCo consists of two algorithms for each safety message, e.g., CAM and DENM.

Contributions of *CoCo* are summarized as follows:

- Considering the characteristics of two safety messages, we propose a distributed congestion control scheme, called CoCo, that consists of two algorithm for each safety message and minimizes the performance degradation of CAM and DENM traffic when congestion problems occur in C-V2X communications.

- The proposed scheme is a very feasible solution to mitigate congestion problems because it does not require hardware modification or any signal exchange. More importantly, it is standard compliant.

- We evaluate performance of the proposed scheme via simulation which reflects realistic vehicle mobility and road situations based on Simulation of Urban MObility (SUMO) [31].

With these contributions, UEs reduce their congestion problem by adjusting their transmission according to their situations.

1.3.3 IDC-aware resource allocation based on multi-agents reinforcement learning

We provide a IDC-aware resource allocation based on multi-agents reinforcement learning that aims to select a clean radio resource while mitigating damages by IDC problem. We claim the following major contributions:

- We model a realistic IDC interference between LTE and NR at ITS band.
- We formulate a IDC-aware resource allocation as a multi-agent reinforcement learning that each UE collects local observations and selects an action and then achieves a reward.
- We confirm that the multi-agents successfully learn their policies and achieves higher Packet Delivery Ratio (PDR) performances compared to the legacy scheme.

1.4 Organization of the Dissertation

The rest of the dissertation is organized as follows.

Chapter 2 presents a feedback mechanism for D2D communication and groupcast rate adaptation. Philosophies for desiging the feedback mechanism are introduced and a detail procedure of the groupcast rate adaptation algorithm is provided. The performances of the proposed groupcast rate adaptation algorithm are validated through extensive simulation evaluations.

In Chapter 3, we present *CoCo*, context-aware congestion control scheme for LTE-V2V communications. First, we provide the reasons why the congestion problem can occur frequently. Next, we present the congestion control scheme for CAM, which adjusts the transmission interval of CAM according to the status change rate of UE.

Then, we also present the congestion control scheme for DENM, which determine whether to transmit or not depending on UE's status. The performance of *CoCo* is evaluated in various scenarios with comparison schemes.

Chapter 4 presents IDC-aware resource allocation based on multi-agents reinforcement learning. We first present a realistic modeling of IDC interference between LTE and NR based on spectrum emission mask specified at the standard. Then, we explain how to formulate a IDC-aware resource allocation as a multi-agent reinforcement learning that each UE collects local observations and selects an action and then achieves a reward. We evaluate the performance of the proposed resource allocation scheme compared to the legacy scheme.

Finally, Chapter 5 concludes the dissertation with the summary of contributions and discussion on the future work.

Chapter 2

Efficient feedback mechanism for LTE-D2D communication

2.1 Introduction

Along with the widespread use of smartphones and the development of wireless communication technologies, the amount of data traffic has soared dramatically. Cisco expects that global mobile data traffic will increase almost eightfold between 2015 and 2020 [32]. In order to support such increased traffic, Long Term Evolution (LTE)-based Device-to-Device (D2D) communication has been considered a key traffic offloading technology. Since User Equipments (UEs) communicate with other UEs directly, the spectral efficiency can be significantly enhanced.

In this paper, we consider D2D communication protocol recently developed in 3GPP [33].[1] In 3GPP D2D, only groupcast (or multicast)-based communication is supported, where D2D Transmitter (Tx) groupcasts data traffic to multiple D2D Receivers (Rxs) (belonging to the same group). However, feedback mechanism between D2D Tx and D2D Rxs is not defined. In fact, it is difficult to define a feedback mechanism without incurring high signaling overhead because multiple channels exist between D2D

[1]We refer to LTE-based D2D communication as *D2D communication* for convenience for the rest of the paper.

Tx and D2D Rxs. Due to the lack of feedback mechanism, D2D Tx cannot acquire the channel quality information, thus making it difficult to use radio resources efficiently.

We first propose feedback channel to support feedback mechanism between D2D Tx and D2D Rxs. In order for D2D Rxs to transmit feedback to D2D Tx, they need resources that are normally assigned and announced by Base Station (BS) or D2D Tx. The incurring signaling overhead should be proportional to the number of Rxs. In our feedback mechanism, the feedback resource location is implicitly determined by the resource location of the control signal from D2D Tx, which is used for the announcement of the Tx's data transmission. By doing so, we completely remove the signaling overhead for feedback resource assignment. The proposed feedback channel also allows multiple D2D Rxs to transmit feedback in one Resource Block (RB)[2] using different cyclic shifted versions of a sequsence, which have good auto-correlation property. Therefore, the proposed feedback channel can use radio resources efficiently.

On top of the proposed feedback mechanism, we propose a rate adaptation algorithm for D2D communication. As mentioned above, D2D communication supports only groupcast. Considering the existence of multiple D2D Rxs, the proposed rate adaptation algorithm aims to adjust Modulation and Coding Scheme (MCS) level according to the performance of the D2D Rx with the worst channel quality. The proposed rate adaptation algorithm is also designed in consideration of possible problems that can occur in D2D communication, e.g., in-band emission. We also propose a retransmission scheme on the proposed feedback mechanism to support an application, which need retransmission, such as file download.

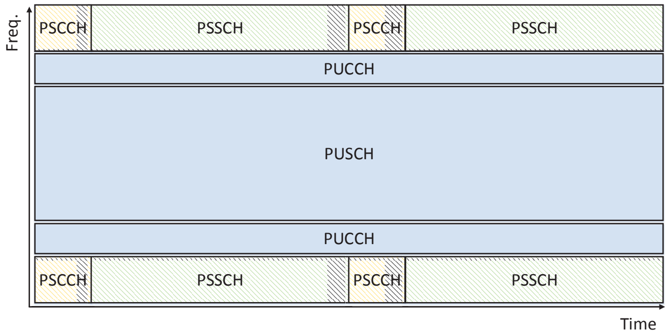

Figure 2.1: An illustration of physical resource pool for LTE-based D2D communications.

2.2 Background

2.2.1 Background for D2D

3GPP defines the basic framework for D2D communication as follows [33]. First, D2D uses dedicated physical resources, separate from cellular uplink resources. Second, D2D supports only groupcast without feedback mechanism. To compensate for the absence of feedback mechanism, blind retransmission is adopted, i.e., Tx transmits packets repeatedly regardless of whether Rx receives the packets or not. 3GPP also defines physical channels for D2D. In Fig. 2.1, Physical Uplink Shared CHannel (PUSCH) for uplink data transmission is located in the middle of the frequency band and Physical Uplink Control CHannel (PUCCH) for control packet transmission is located at both ends of PUSCH.

Physical Sidelink Control CHannel (PSCCH) is additionally defined for Scheduling Assignment (SA) transmission in D2D communication. SA is control information periodically transmitted before data transmission and contains information including group ID, MCS level, and resource location for data transmission. Physical Sidelink Shared CHannel (PSSCH) is also additionally defined for data transmission in D2D

[2] One RB consists of 84 resource elements, composed of 12 subcarriers and seven symbols.

communication. In Fig. 2.1, PSCCH and PSSCH are located at both ends of PUCCH. PSCCH and PSSCH regions are repeated periodically, where the length of the period is out of 40, 80, 160, and 320 ms.

3GPP D2D supports two resource access modes. In mode 1, BS allocates resources, e.g., PSCCH and PSSCH, to D2D Txs requesting resource allocations. Therefore, in mode 1, there is no resource collision among D2D Txs. However, in mode 2, since D2D Txs randomly select resources within a predefined resource pool, there could be a resource collision among D2D Txs. SA transmitted via PSCCH contains essential information for data transmission and reception as stated above. Therefore, if D2D Rx does not receive SA due to resource collision, the D2D Rx can not receive data from D2D Tx in that period. In this paper, we consider that resource allocations for SA always follow mode 1, but, resource allocations for D2D data can follow both modes 1 and 2. where all D2D UEs do not suffer from resource collision.

2.2.2 UE Behaviors in D2D

D2D UE behaves as follows. First, BS allocates resources, e.g., PSCCH and PSSCH, to D2D Tx. Through the allocated resources, the D2D Tx transmits both SA and data two and four times, respectively, due to the blind retransmission. Since D2D Rx does not know what resources the D2D Tx uses, the D2D Rx blindly decodes PSCCH resource pool and checks if the group ID of the decoded SA matches its own ID. If they match, the D2D Rx decodes data based on the decoded SA. Otherwise, the D2D Rx waits until the next PSCCH resource pool.

Using Fig. 2.2, we explain D2D UE behaviors in D2D communication. There are two groups, i.e., groups A and B. Firstly, BS allocates resources, e.g., PSCCH and PSSCH, to D2D Tx in group A. Fig. 2.2a shows that the D2D Tx transmits SA two times via assigned resources, and D2D Rxs blindly decode PSCCH resource pool and check the ID of the decoded SA. D2D Rxs in group A find the matching ID, while D2D Rx in group B does not. Therefore, Fig. 2.2b shows that D2D Rxs in group A decode data and D2D Rx in group B waits for the next PSCCH resource pool.

2.2.3 Time Repetition Pattern for Transmission

As mentioned above, SA contains resource location for data transmission, i.e., locations of frequency resource and time resource. location of Frequency resources is explicitly recorded in SA, but, location of time resources is implicitly recorded in SA by Time Repetition Pattern for Transmission (T-RPT). T-RPT is a pattern that informs the transmission time in time resources and it is expressed by 8 bit bitmap for indicating time resources.

In T-RPT, one bit indicates whether to transmit or not in one subframe (1 ms). So, one T-RPT indicates the subframe to transmit during 8 ms and T-RPT repeats until PSSCH resource pool is finished. Therefore, through T-RPT, Tx and Rx can know location of time resources. For example, we assume that the length of the period is 80 ms, i.e., the amount of times for PSCCH and PSSCH are 4 ms and 76 ms, respectively. Fig. 2.3 shows an example of T-RPT. Allocated T-RPT is 1 1 0 0 0 1 1 0 and the T-RPT repeats nine times completely until PSSCH resource pool is finished. After the nine repetitions, 4 ms remains. In that case, T-RPT is truncated by 4 ms, i.e., truncated T-RPT is 1 1 0 0, and then indicates subframes for 4 ms. Therefore, there are 38 transmission times and nine Transport Blocks (TB) are transmitted four times. The last TB is transmitted two times due to truncated T-RPT.

2.2.4 Related work

The authors of [9] propose a rate adaptation scheme for D2D communication in groupcast scenarios. However, as mentioned above, satisfying the assumption should be difficult. Actually, very few studies have proposed rate adaptations for D2D communication. However, in other research areas, there are many papers for rate adaptation in multicast scenarios. (See the survey in [34], for example.)

In cellular networks, Araniti *et al.* [35] propose a subgrouping technique for mul-

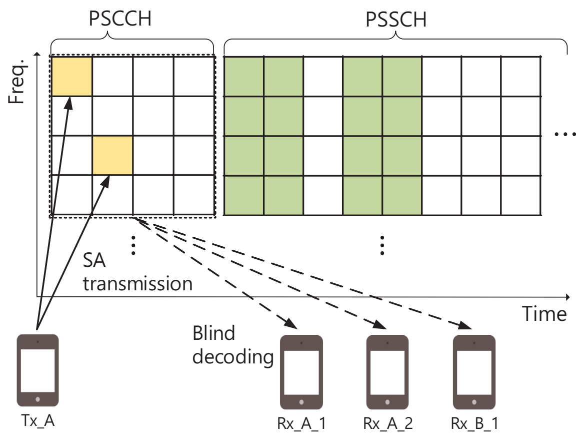

(a) SA transmission and reception.

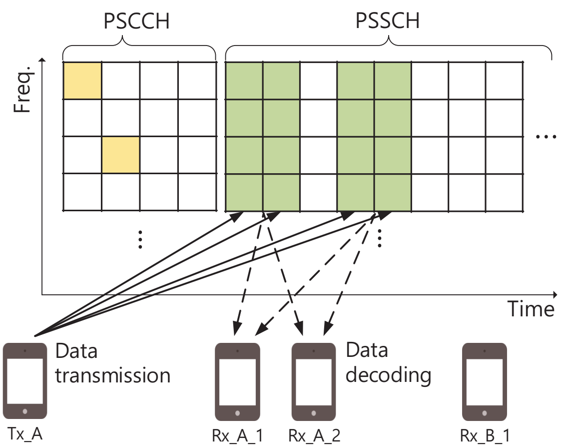

(b) Data transmission and reception.

Figure 2.2: Behaviors of UEs in D2D communication: (a) SA transmission and reception and (b) Data transmission and reception.

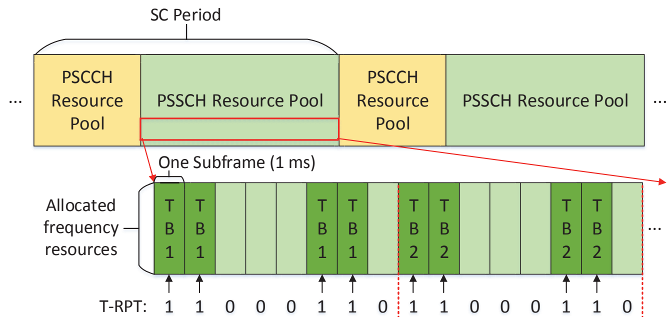

Figure 2.3: An example of time repetition pattern for transmission.

ticast rate adaptation in LTE. The subgrouping technique is to group multicast Rxs into subgroups of Rxs experiencing similar channel quality for efficient data transmissions. In the downlink of cellular communications, BS is the only Tx. Therefore, the subgrouping based on channel quality between the fixed Tx, i.e., BS, and Rxs does not incur a large overhead. However, in D2D communication, Tx is not fixed, but can change at any time. Therefore, the subgrouping technique can cause a large overhead in D2D communication since subgrouping is required every time Tx changes.

Gupta *et al.* [36] introduce multicast rate adaption schemes in Wireless Local Area Network (WLAN). The simplest multicast rate adaptation scheme introduced in the paper requires all Rxs to transmit feedback. This approach is simple, but it is inefficient because all Rxs should send feedback. Leader-based scheme and cluster-based scheme are introduced in [36] as techniques for solving such inefficiency. In leader-based scheme, a leader is elected, i.e., the Rx with the worst channel quality among all Rxs becomes the leader, and the leader sends feedback to the Access Point (AP) on behalf of the group. In cluster-based scheme, clusters are created based on location, and the Rx with the worst channel quality in a cluster becomes the head of the cluster. The head transmits feedback to the AP on behalf of its cluster.

In WLAN, since the entity receiving feedback is fixed as AP, leader election and clustering do not incur large overhead. However, in D2D communication, as mentioned above, since the entity receiving feedback can be changed at any time, both cluster-based scheme and leader-based scheme can cause significant overhead.

There are studies [37–40], which consider retransmission of D2D communications. However, in the studies [37, 38], the authors assume the situation where D2D UEs retransmit packets for cellular downlink traffic. On the other hand, we consider retransmission for D2D data traffic ,which is generaged by D2D UEs. In the studies [39, 40], the authors consider retransmission via relay node. Khoueiry *et al.* [39] propose a network coding strategy to enhance multicast performance. However, the author of [39] consider that topology is fixed and relay node is also fixed. As mentioned above, in D2D communications, Tx is not fixed, but can change at any time. Therefore, fixed relay node is impractical since the quality of radio channel changes each time Tx changes.

Zhou *et al.* [40] also propose D2D relay algorithm. the author assumes that BS multicasts data ,then D2D UEs, which received the data, retransmit the data. The proposed algorithm requires resource allocations for the potential relay nodes. Therefore, the solution might be not scalable if there are many UEs. There are many studies [41–47] for retransmission in other communication systems, e.g., cellular networks and WLAN.

In most studies [41–47] for retransmission via network coding. The authors assume that the links, i.e., radio resources, between Tx and all Rxs are already setup. Therefore Rx transmits feedback for retransmission request via allocated link and then Tx efficiently retransmits encoded packets based on feedback. However, the assumption that radio resources for feedback are already setup should be difficult because resource allocations for D2D Rxs are not scalable if there are many D2D Rxs.

2.3 System model

In this section, we explain the target system model assuming that D2D UEs communicate with each other. We consider multicell scenarios with seven cells, where there

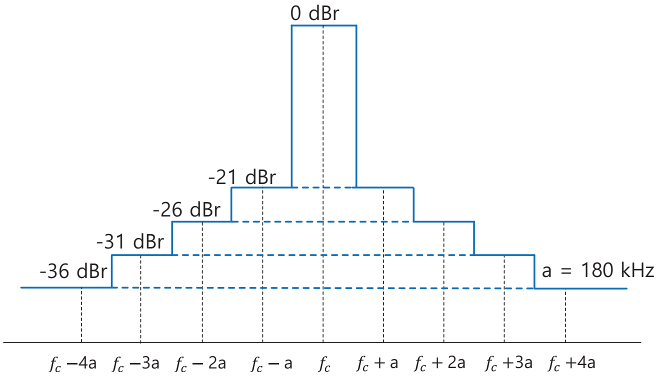

Figure 2.4: Spectral mask of in-band emission.

are N D2D groups for each cell. Each D2D group consists of M D2D UEs, and D2D Txs groupcast data to their group members. In 3GPP standard [33], the groups, performing D2D communication, are formed in advance and the information of group formations is initially known through a D2D service authorization, which is mandatory to use D2D services. Accordingly, we assume that D2D UEs know the own group information since the D2D UEs perform the D2D service authorization.

We assume that D2D Txs in the same group do not transmit SA using the same time resource, i.e., the same subframe, in order to receive all SAs sent from the same group. Since we consider mode 1 D2D, in which BS allocates resources to D2D Txs, the assumption is feasible. Resource pools, e.g., PSCCH and PSSCH, are periodically repeated, and we assume that the period is 80 ms, one of the options in the 3GPP standard.

We also consider in-band emission, which is unwanted power leakage from the allocated bandwidth for transmission to the unallocated bandwidth within the total bandwidth used by the network operator. Fig. 2.4 shows spectral mask of in-band emission caused by transmission via one RB, i.e., bandwidth of 180 kHz, according to Clause A.2.1.5 of [48]. As shown Fig. 2.4, at the ±180 kHz from the center frequency, (f_c), transmission power is attenuated by 21 dB, i.e., the RBs closest to the allocated RB experience 21 dB attenuated power leakage at the transmission power. The far-

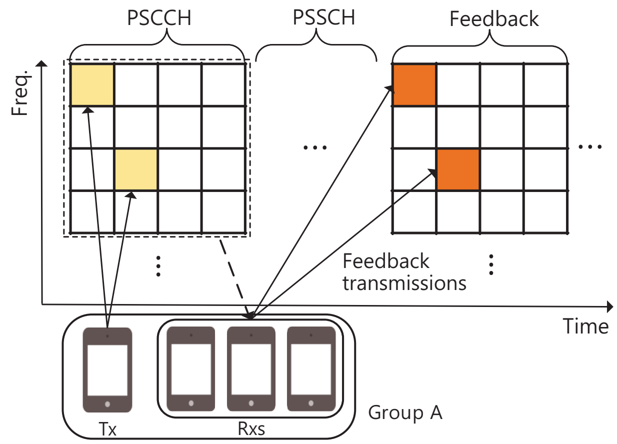

Figure 2.5: An example of the proposed feedback mechanism for D2D communication.

ther away from the center frequency, the less the unwanted power leakage. Thus, RBs adjacent to the assigned RB are more susceptible to in-band emission.

In the uplink of cellular communication, BS is the only Rx. Since BS can adjust transmission power of a UE based on the channel quality between BS and the UE, received power levels at BS can be similar. Therefore, in-band emission problem is not severe in cellular communication because the ratio of the attenuated power incurred by in-band emission to the power of the target signal can be relatively small. However, in D2D communication, unlike the uplink of cellular communication, there are multiple D2D Rxs. Since it is difficult to control transmission power based on any one D2D Rx, D2D Tx transmits signal with maximum power. As a result, the ratio of the attenuated power incurred by in-band emission to the power of the target signal can be large enough to affect D2D communication. We use a realistic system model to evaluate the impact of in-band emission in D2D communication.

2.4 Feedback Mechanism

We consider two philosophies for designing a feedback mechanism for D2D. First, we try to allocate as few resources as possible to the feedback channel in order to minimize the waste of resources used for the feedback channel. Second, D2D Rx should be able to use the proposed feedback mechanism regardless of its connection with BS. In general, D2D Rxs do not need to be connected to BS because they can directly receive data from D2D Txs. Therefore, feedback mechanisms that can be used only through BS are not desirable.

We propose that D2D Rxs transmit feedback using the RBs at the same positions as SAs transmitted by the D2D Tx belonging to the same group. Fig. 2.5 shows an example of our proposed feedback mechanism. As shown in the figure, D2D Tx transmits SA containing the information for data reception twice via PSCCH, and D2D Rxs, belonging to the same group, blindly decode PSCCH resource pool and receive two SAs transmitted by the D2D Tx. Since the position of feedback resource is the same as the position of the SA transmitted in the same group, the D2D Rxs transmit the feedback at the received SA resource locations without additional signaling, i.e., without additional signaling, two RBs are assigned to D2D Rxs and D2D Rxs transmit the feedback.

In order to allow multiple D2D Rxs to use the limited feedback resources, i.e., two RBs, we use cyclic shifted versions of a sequence with good auto-correlation property. When such a sequence is cyclic shifted, the shifted sequence and the original sequence are nearly orthogonal. By using the property, up to 12 D2D Rxs can use one RB simultaneously.[3] Therefore, when D2D Rxs transmit feedback only once, 24 D2D Rxs can transmit feedback using two RBs. In this paper, we use Zadoff-Chu sequences, which are known to have ideal auto-correlation property, with length 12. Since 3GPP considers the number of group members to be around 10 in general scenarios [48], the proposed feedback channel should be able to support all the group members.

There are two issues, which we have to address. The first issue is near-far problem since the proposed feedback channel allows multiple D2D Rxs to use the same resources at the same time. We briefly explain near-far problem through an example.

[3] Since one RB spans 12 subcarriers, a sequence of length 12 is used for one RB.

Near D2D UE and far D2D UE transmit feedback to a D2D Tx via the same feedback resource. Then the D2D Tx receives feedback and conducts AGC. In AGC, both feedback signals are multiplied by a common gain. The common gain depends on the strong signal because the received signal must not go out of the dynamic range of the ADC. At that time, the weak signal might become indistinguishable from quantization noise because the weak signal becomes too small.

We apply Open Loop Power Control (OLPC) to D2D communications to mitigate near-far problem. Through OLPC, D2D Rxs adjust transmission power based on the strength of the received signal from D2D Tx belonging to the same group. Through simulation results in Section 2.6, we confirm the effect of near-far problem on the proposed feedback channel and how the effect of near-far problem on the proposed feedback channel changes when OLPC is applied.

As mentioned in Section 2.3, the in-band emission is the second issue. Since the proposed feedback channel allows multiple D2D Rxs to use one RB, the in-band emission caused by multiple D2D Rxs can accumulate. Therefore, D2D Tx may fail to receive feedback due to an accumulated in-band emission. On top of the proposed feedback channel, we propose a groupcast rate adaptation algorithm, which tries to mitigate the damage caused by the accumulated in-band emission, and a retransmisssion scheme, which can utilize the proposed feedback mechanism.

The proposed feedback mechanism has several advantages. Above all, since feedback resources are assigned to D2D Rxs via SAs sent from the same group, D2D Rxs can use the proposed feedback mechanism without the help of BS. Therefore, no additional signaling is required for feedback scheduling. Second, the overhead of using feedback resources can be reduced because multiple D2D Rxs transmit feedback using one RB. In summary, we propose an efficient feedback mechanism that minimizes the overhead, i.e., the amount of feedback resources, and signaling for feedback resource scheduling.

Table 2.1: Notations and parameters used in pseudo codes.

Symbol	Definition
$SA_{i,j}$	SA located at ith subframe and jth RB
$MCS_{i,j}$	MCS level within $SA_{i,j}$
$ID_{i,j}$	Group ID within $SA_{i,j}$
ID_m	Group ID of the mth D2D UE
M_n	MCS level used in nth period
$FM_{n,m}$	MCS level from the mth UE in nth feedback transmission
N_{time_PSCCH}	The number of subframes for PSCCH
N_{freq_PSCCH}	The number of RBs at a given subframe for PSCCH
FI	Feedback sensing indicator
γ_{data}	SINR of received data
fm	Maximum supportable MCS level
K	The number of group members
Th	BLER threshold
$F_{rsc_{1st}}$	Set of feedback successfully received via 1st feedback resource
$F_{rsc_{2nd}}$	Set of feedback successfully received via 2nd feedback resource
F	Set,combined $F_{rsc_{1st}}$ and $F_{rsc_{2nd}}$

2.5 Groupcast Rate Adaptation Algorithm

On top of the proposed feedback channel, we propose a groupcast rate adaptation algorithm, called Fast and Robust Rate Adaptation (FaRRA) algorithm. FaRRA is an algorithm for D2D Rxs to effectively transmit feedback while trying to reduce in-band emission in the proposed feedback channel. In FaRRA algorithm, D2D Rxs, which want to raise MCS level, opportunistically transmit feedback to reduce in-band emission. However, D2D Rxs desiring to lower MCS level transmit feedback twice so that D2D Tx can receive the feedback successfully. FaRRA algorithm conservatively operates by giving the priority to feedback requesting to lower MCS level in order to satisfy all group members, and tries to increase the spectral efficiency, e.g., bits/Hz, by making D2D Rxs opportunistically transmit feedback requesting to raise MCS level.

Table 2.1 lists notations and parameters used in the pseudo codes for algorithms. Algorithm 1 provides the behavior of D2D Rx with FaRRA algorithm. The D2D Rx

Algorithm 1 Rx's behavior of FaRRA algorithm

Set:
1: $FI = 0$ {feedback sensing indicator}
2: $fm = 0$ {supportable MCS level}
3: m {ID of D2D Rx in consideration}
During nth SA transmission: $i \leftarrow 1, \cdots, N_{time\_PSCCH}$ $j \leftarrow 1, \cdots, N_{freq\_PSCCH}$ $ID_m == ID_{i,j}$
4: receive SA
5: $M_n \leftarrow MCS_{i,j}$
During nth data transmission: receive SA
6: receive data
7: $\gamma \leftarrow E[\gamma_{data}]$ $TBLER(\gamma, fm) \leq Th$
8: $fm = fm + 1$
9: $FM_{n,m} \leftarrow fm$
During nth feedback transmission: $FM_{n,m} \geq M_n + 1$
10: monitor $1st$ feedback resource sense feedback of receivers
11: $FI = 1$ $FI == 0$
12: transmit feedback via $2nd$ resource $FM_{n,m} < M_n + 1$ && $FM_{n,m} \geq M_n$
13: transmit feedback via $1st$ resource
14: transmit feedback via $1st$ and $2nd$ resources

sets FI and fm to 0 before the nth period begins (lines 1–2). During the nth SA transmission (lines 4–11), the D2D Rx blindly decodes the entire PSCCH resource pool and compares the ID of the decoded SA with its own ID. If there is an SA with the ID matching its own ID, the D2D Rx fully receives SA and checks the information in the SA including MCS level and resource location of data transmission. During the nth data transmission (lines 12–19), the D2D Rx receives data via PSSCH. The D2D Rx determines the average SINR of the received data, and finds the highest MCS level that limits Transport Block Error Rate (TBLER), which is the ratio of the number of erroneous transport blocks (TBs) to the total number of TBs, to the predefined threshold. The D2D Rx calculates TBLER using MCS level and the average SINR of data signal, i.e., γ, and the highest MCS level is fed back by the D2D Rx to D2D Tx.

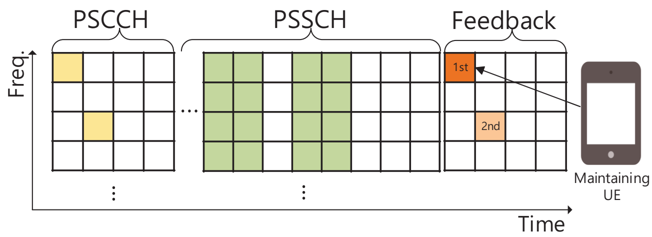

(a) Rx to maintain MCS.

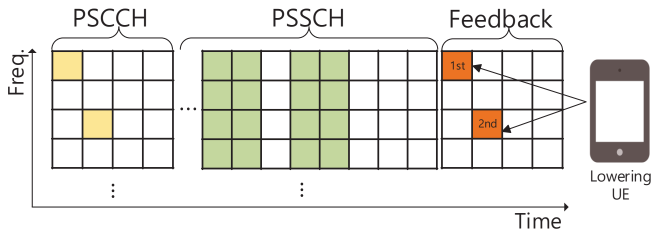

(b) Rx to lower MCS.

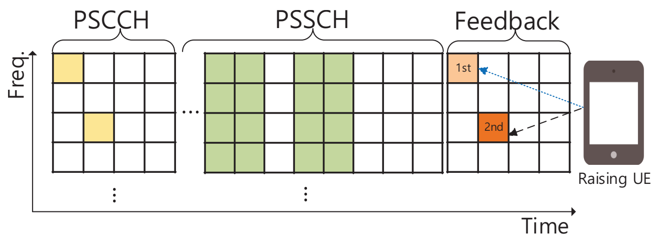

(c) Rx to raise MCS.

Figure 2.6: D2D Rx behavior of FaRRA algorithm: (a) Rx to maintain MCS, (b) Rx to lower MCS, and (c) Rx to raise MCS.

During the nth feedback transmission (lines 20–34), D2D Rx is classified into one of three types, i.e., D2D Rx which wants to raise MCS level, that to maintain MCS level, and that to lower MCS level. In case of D2D Rx, desiring to raise MCS level (lines 20–27), the D2D Rx monitors whether other D2D Rxs send feedback via the first feedback resource (in the chronological order). If feedback from another D2D Rx is detected, FI is set to 1 and the D2D Rx does not transmit feedback in the nth feedback transmission. Otherwise, the D2D Rx sends $FM_{n,m}$ to D2D Tx via the second feedback resource. In case of D2D Rx, desiring to maintain MCS level (lines

Algorithm 2 Tx's behavior of FaRRA algorithm

Set:

M_n {MCS level used in nth period}

K {the number of group members}

$F_{rsc_{1st}} = \emptyset$ {received feedback set}

$F_{rsc_{2nd}} = \emptyset$ {received feedback set}

During nth feedback period via 1st resource:

receive feedback of kth Rx

$F_{rsc_{1st}} \ni FM_{n,k}$

During nth feedback period via 2nd resource:

receive feedback of kth Rx

$F_{rsc_{2nd}} \ni FM_{n,k}$

Rate adaptation for (n+1)th period:

$F_{rsc_{1st}} == \emptyset \parallel F_{rsc_{2nd}} \parallel == K$

$M_{n+1} \leftarrow \min(F_{rsc_{2nd}})$

$M_{n+1} \leftarrow M_n + 1$ $F_{rsc_{2nd}} == \emptyset$

$M_{n+1} \leftarrow M_n$

$F \leftarrow combining\ F_{rsc_{1st}}\ and\ F_{rsc_{2nd}}$

$M_{n+1} \leftarrow \min(F)$

28–30), the D2D Rx transmits $FM_{n,m}$ to D2D Tx via only the first feedback resource. D2D Rx, which wants to lower MCS level, always transmits $FM_{n,m}$ to D2D Tx two times by using both the first and second feedback resources.

Because D2D supports only groupcast, feedback requesting to lower MCS level is given the highest priority while feedback requesting to raise MCS level is given the lowest priority to support all the group members reliably. Therefore, in FaRRA algorithm, D2D Rxs, desiring to lower MCS level, preferentially transmit their own feedback two times via two feedback resources. Feedback requesting to raise MCS level becomes meaningless if D2D Tx receives feedback requesting to lower or maintain MCS level. In this case, if feedback requesting to raise MCS level is transmitted, it just worsens in-band emission problem. Accordingly, D2D Rxs, which want to raise MCS level, transmit their feedback via the second feedback resource only when the feedback is meaningful.

Fig. 2.6 shows an example for feedback transmission of D2D Rx. Firstly, feedback resources, i.e., two RBs, are assigned to D2D Rx by SA sent from D2D Tx. Fig. 2.6a shows feedback transmission of D2D Rx, desiring to maintain MCS level in FaRRA algorithm. Since feedback requesting to maintain MCS level can be expressed in a single bit, there is less need to increase SINR of the feedback for successfully decoding the feedback. Therefore, the D2D Rx transmits feedback via only the first feedback resource. It also helps relieve in-band emission problem by decreasing the number of feedback transmissions. As shown in Fig. 2.6b, D2D Rx, desiring to lower MCS level, transmits feedback twice using two feedback resources to increase SINR of the feedback because the improved SINR of the feedback increases the probability of successfully feedback decoding by D2D Tx.

The behavior of D2D Rx, desiring to raise MCS level, is shown in Fig. 2.6c. First, the D2D Rx monitors the first feedback resource to check the transmission of feedback requesting to lower or maintain MCS level. If the D2D Rx senses such feedback, the D2D Rx abandons transmission of its feedback requesting to raise MCS level in order to avoid unnecessary in-band emission due to the second feedback resource. Otherwise, the D2D Rx transmits feedback requesting to raise MCS level via the second feedback resource.

Algorithm 2 provides a description of the D2D Tx behavior in FaRRA algorithm. D2D Tx determines M_n, checks K, and sets $F_{rsc_{1st}}$ and $F_{rsc_{2nd}}$ to empty sets before the nth period begins (lines 1–4). During the nth feedback transmission via the first feedback resource (lines 5–7), the received feedback is put into $F_{rsc_{1st}}$. On the contrary, the received feedback via the second feedback resource is put into $F_{rsc_{2nd}}$ (lines 8–10).

During rate adaptation for the $(n+1)$th period (lines 11–24), D2D Tx first checks $F_{rsc_{1st}}$. If $F_{rsc_{1st}}$ is an empty set, the D2D Tx checks $F_{rsc_{2nd}}$. If the cardinality of $F_{rsc_{2nd}}$ is the same as the number of group members, the D2D Tx adapts the lowest MCS level based on $F_{rsc_{2nd}}$ (lines 11–13). Otherwise (lines 14–16), it means that the D2D Tx did not receive feedback from all D2D Rxs in the group. Therefore, in this case, the D2D Tx conservatively raises MCS level by one. If $F_{rsc_{1st}}$ is not an empty set, there exist demands for lowering or maintaining the current MCS level (lines 17–24). When $F_{rsc_{2nd}}$ is an empty set, the D2D Tx maintains the MCS level because there are only D2D Rxs, which want to maintain MCS level (lines 18–19). Otherwise, $F_{rsc_{1st}}$ and $F_{rsc_{2nd}}$ are combined to increase the SINR of the feedback signal, and then the D2D Tx determines the lowest MCS level based on F, obtained by combining $F_{rsc_{1st}}$ and $F_{rsc_{2nd}}$ (lines 20–24).

We additionally consider two more algorithms to compare with FaRRA algorithm. The first comparison algorithm is In-band Emission (IE) algorithm, in which all D2D Rxs send feedback through feedback resources regardless of the purpose, i.e., lowering, maintaining, or raising MCS level, and D2D Tx selects MCS level for the next period based on the received feedback. FaRRA algorithm tries to reduce the number of D2D Rxs transmitting feedback as much as possible considering the damage caused by in-band emission. On the other hand, the number of feedback-transmitting Rxs remains constant with IE algorithm, i.e., all D2D Rxs always transmit feedback during the period of feedback transmission. We compare the effectiveness of FaRRA algorithm, which reduces the number of D2D Rxs transmitting feedback, with IE algorithm.

The second comparison algorithm is Robustness Oriented (RO) algorithm, which focuses on successful data reception of all members. RO algorithm works in the same way as FaRRA algorithm during SA and data transmission. However, in RO algorithm, two turns, i.e., MCS level lowering turn and MCS level raising turn, are repeated altenately. In a MCS level lowering turn, only D2D Rxs, desiring to lower MCS level, transmit feedback and D2D Tx determines MCS level based on the received feedback. In a MCS level raising turn, both types of D2D Rxs, i.e., desiring to lower and desiring to maintain MCS level, transmit feedback and D2D Tx decreases or maintains MCS level if the D2D Tx receives feedback, which requests to decrease or maintain MCS level. If D2D Tx does not receive any feedback, the D2D Tx increases MCS level by one because all group members agree to raise MCS level.

FaRRA algorithm tries to reduce the amount of in-band emission by transmitting feedback requesting to raise MCS level opportunistically. However, RO algorithm

Table 2.2: Simulation environments.

Carrier frequency	2 GHz
System bandwidth	10 MHz (50 RBs)
Topology	Uniform distribution
Channel model	Fast fading + shadowing + pathloss + in-band emission [48]
The number of bits for ADC	12 bits
Transmission power	23 dBm
Noise figure	9 dB
Noise power	-174 dBm/Hz

has a large advantage in reducing the amount of in-band emission because D2D Rxs, which want to raise MCS level, do not transmit feedback at all at the cost of delayed MCS level increase. We investigate the robustness of FaRRA algorithm over in-band emission by comparing FaRRA algorithm with RO algorithm.

2.6 Performance Evaluation

In this section, we evaluate the impact of near-far problem over the proposed feedback channel and the performance of FaRRA algorithm. We also evaluate the performance of feedback-aided retransmission on top of the proposed feedback mechanism. We follow the evaluation methodology in Annex A.2 of [48] for our system level simulation using MATLAB. In this simulation, we assume that the system bandwidth is 10 MHz, which can accommodate up to 50 RBs in frequency domain, and the period is 80 ms consisting of 4 ms for PSCCH and feedback and 72 ms for PSSCH.

2.6.1 Simulation Environments

Table 2.2 summarizes the simulation environments, and details are described below.
Topology: We consider multicell scenarios with seven cells and the radius of each cell is 150 m. There are three groups of UEs in each cell. A group consists of one Tx and nine Rxs. Txs are randomly distributed in a cell. Rxs are also randomly distributed around the Tx belonging to the same group.

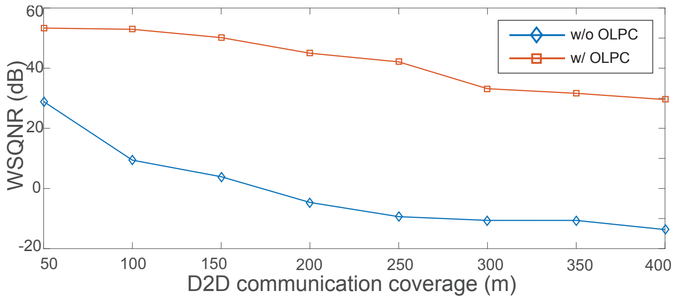

Figure 2.7: Impacts of near-far problem.

Channel model: We consider fast fading generated using ITU-R IMT UMi model [49]. We also create shadowing following a log-normal distribution with standard deviation of 3 dB as specified in Clause A.2.1.2 of [48]. Pathloss is calculated using WINNER+B1 model [50]. Finally, in-band emission is also generated according to Clause A.2.1.5 of [48].

Near-far problem: The proposed feedback channel allows multiple Rxs to use the same feedback resource. Therefore, when near Rxs and far Rxs (from a given Tx) transmit feedback simultaneously, the Tx can suffer from near-far problem. All received signals are multiplied by a common gain and enter Analog-to-Digital Convertor (ADC), which uses 12 bits to quantize signals. Quantization level is determined by the sum of power levels of received signals, and determines quantization noise. Throughout simulations, we consider the quantization noise when calculating SINR.

2.6.2 Impact of Near-Far Problem

We first evaluate the impact of near-far problem on the proposed feedback channel. For simplicity, we assume that there are one D2D Tx and two D2D Rxs, i.e., a near D2D Rx and a far D2D Rx, and then the D2D Rxs transmit feedback via the same feedback resource. We consider a performance metric, called Weakest received Signal strength to Quantization Noise Ratio (WSQNR), which is the ratio of signal strength of the far D2D Rx to quantization noise. Since the signal from the far D2D Rx is more susceptible to the quantization noise than that of the near D2D Rx, it is meaningful to check WSQNR performance.

Fig. 2.7 shows the WSQNR performance both when OLPC is applied and when it is not, depending on D2D communication coverage, which means the radius in which D2D Tx can handle D2D communication. We first observe that the WSQNR performance unacceptably degrades, e.g., even under 0 dB, as the D2D communication coverage increases when OLPC is not employed. Therefore, without OLPC, it is difficult to use the proposed feedback channel, especially, when we target large D2D communication coverage. On the other hand, when OLPC is employed, the WSQNR performance is greatly improved. Accordingly, we conclude that OLPC should be applied to increase D2D communication coverage.

2.6.3 Comparison of Rate Adaptation Algorithms

Now, we evaluate FaRRA algorithm in comparison with IE and RO algorithms. Fig. 2.8a shows that each algorithm adapts MCS level every period. The blue line with diamond markers represents the highest achievable MCS level that D2D Rx with the worst channel quality can support. Therefore, to satisfy all Rxs, MCS level should be chosen smaller than or equal to the MCS level pointed by the diamond marker at each period. We observe that IE algorithm does not properly adjust MCS level by choosing MCS level higher than the highest achievable MCS level many times. It means that in-band emission caused by feedback transmissions of all D2D Rxs has a severely negative impact on the reception of feedback by D2D Tx.

In case of FaRRA and RO algorithms, we observe that most MCS values are less than or equal to the highest achievable MCS level. However, in RO algorithm, since D2D Rx does not transmit the feedback requesting to raise MCS level, it does not use resources efficiently. On the other hand, FaRRA algorithm uses resources more efficiently because D2D Rx opportunistically transmits feedback requesting to raise MCS level.

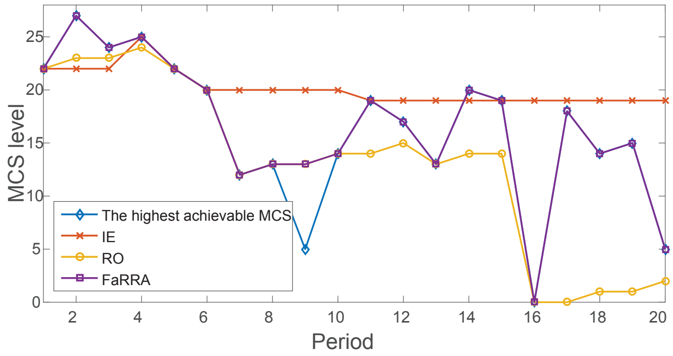

(a) MCS adaptation over time.

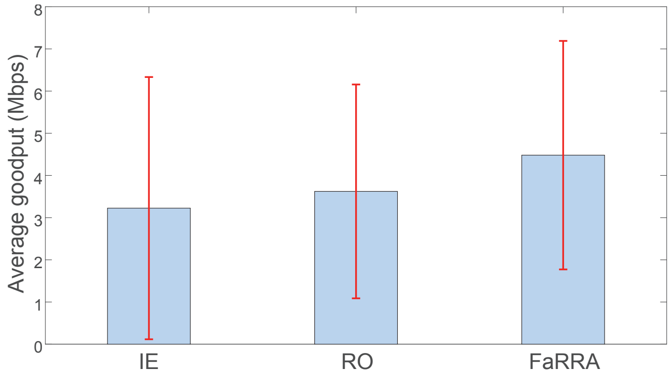

(b) Goodput performance of the worst channel Rx.

Figure 2.8: Comparison of the algorithms: (a) MCS adaptation over time and (b) goodput performance of the worst channel Rx.

Fig. 2.8b shows the average goodput performance of the three algorithms. In case of unicast, goodput is the throughput that Rx successfully received, i.e.,

$$\text{Goodput} = \frac{\#\text{ received blocks } \times \text{block size}}{\text{Period length}} \ (bps).$$

However, we evaluate the throughput that the D2D Rx with the worst channel quality achieves because we consider groupcast scenarios, i.e., we evaluate the goodput of the D2D Rx, which has the worst channel quality in a group. In Fig. 2.8b, FaRRA algorithm achieves higher goodput than the other algorithms. The red bars in Fig. 2.8b represent standard deviations. The standard deviation of FaRRA algorithm is slightly

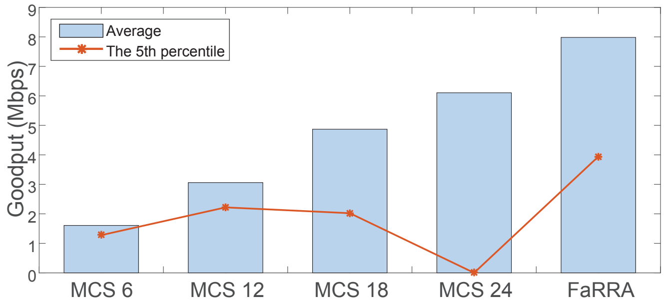

Figure 2.9: Overhead caused by feedback mechanism.

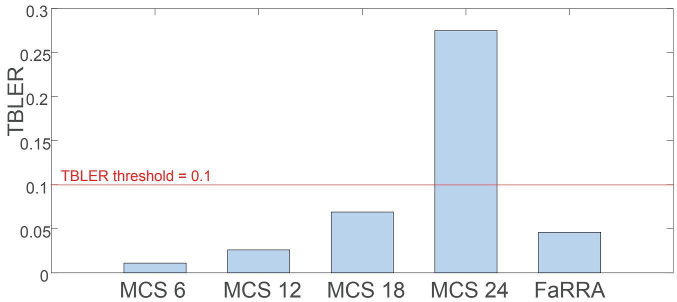

Figure 2.10: Transport block error rate.

larger than that of RO algorithm because FaRRA algorithm is capable of supporting larger MCS level increase compared to RO algorithm. In summary, FaRRA algorithm is as robust as RO algorithm, and, at the same time, it quickly adjusts MCS level, thus enabling more efficient use of radio resources.

2.6.4 Comparison of FaRRA Algorithm and Legacy Scheme

In this subsection, we compare FaRRA algorithm with the legacy scheme using a fixed MCS level. In the legacy scheme, D2D Tx transmits data using a fixed MCS level, e.g., MCS 6, 12, 18, or 24 during PSSCH. In case of the legacy scheme, 4 ms and 76 ms are for PSCCH and PSSCH, respectively. On the other hand, in FaRRA algorithm, D2D Tx adapts MCS level every period, and transmits data for 72 ms since the proposed feedback channel is added, i.e., the reduced 4 ms is for the proposed feedback channel.

Fig. 2.9 shows the goodput obtained by averaging the results from 100 simulation runs. We observe that FaRRA algorithm outperforms the legacy schemes while the legacy scheme with high MCS level tends to achieve higher average goodput. We also observe the 5th percentile goodput, representing the average of the bottom 5% of all goodput performances. We observe that the 5th percentile goodput of the legacy scheme with MCS 24 is almost zero. This demonstrates the limitation of the legacy scheme, which uses a fixed MCS level irrespective of the channel variation.

The reason why fixed MCS 24 achieves such a bad 5th percentile goodput becomes clearer by evaluating the TBLER performance. Fig. 2.10 shows the result of TBLER for both FaRRA and the legacy schemes. We first observe that the TBLER of fixed MCS 24 is over 0.25, thus resulting in almost zero 5th percentile goodput. For fixed MCSs 6 and 12, although they have good TBLER performance, the 5th percentile and the average goodput performances are low due to small transport block sizes. Therefore, it is difficult to use radio resources efficiently in those cases. On the other hand, FaRRA algorithm works properly by keeping the TBLER under the threshold, which is set to 0.1. That is, our simulation results demonstrate that FaRRA algorithm uses radio resources efficiently while keeping TBLER under the threshold.

2.6.5 Performance of Feedback-Aided Retransmission Scheme

We compare performance of feedback-aided retransmission with that of legacy scheme. In this legacy scheme, D2D Tx transmits the same packets four times due to blind retransmission and the D2D Tx has 38 transmission opportunities, i.e., 10 original packets are transmitted. On the other hand, in feedback-aided retransmission, D2D Tx has 36 transmission opportunities due to feedback transmission and the transmission composes of retransmitted packets, original packets, and encoded packets.

We first evaluate goodput performance of feedback-aided retransmission. As shown Fig. 2.11 Feedback-aided retransmission achieves slightly higher average goodput than that of the legacy scheme. We also observe the 20th percentile goodput, representing

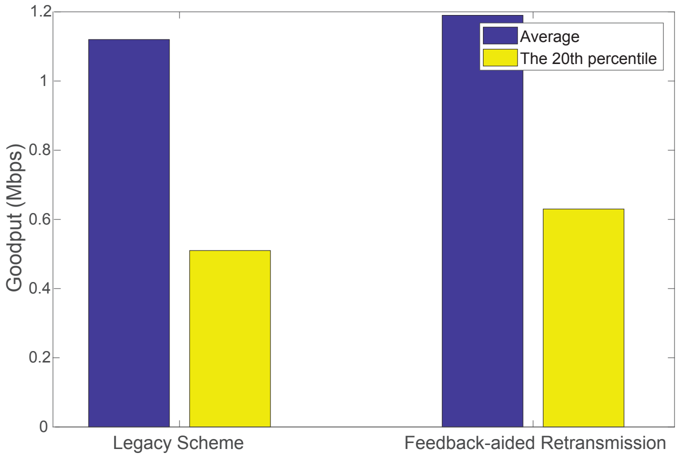

Figure 2.11: Goodput performance of feedback-aided retransmission.

the average of the bottom 20% of all goodput performances. In case of the 20th percentile goodput, feedback-aided retransmission achieves 29% goodput performance gain. Through simulations, we confirm that the blind retransmission works quite robustly, but, among users with low 20% performance, the case that D2D Rxs do not receive packets occurs frequently. This case is relieved by feedback-aided retransmission and the performance gain is obtained.

We also evaluate empirical CDF of file downloading time. The file downloading time is the number of periods used to download the file, completely. We assume that D2D Tx shares about 5 minutes of TED lecture video file[4] with group members via D2D communication during 500 periods. As shown Fig. 2.12, in case of blind retransmission, there are more D2D Rxs that have not completed file download within a given time, i.e., 500 periods. We also observe the 20th percentile performances, representing CDF of the bottom 20% of all file downloading time performances. Through the 20th percentile performances, Feedback aided retransmission achieves higher average file downloading time performance than that of legacy scheme. In case of the

[4]The title of the TED lecture is ”Don’t like clickbait? Don’t click” and the video file size is 31MB.

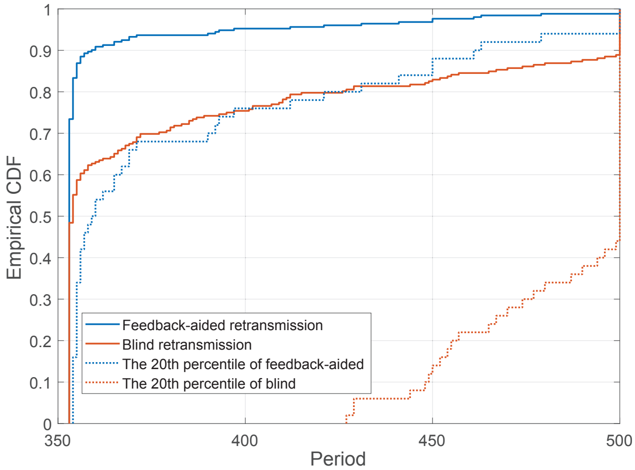

Figure 2.12: Empirical CDF of file downloading time.

20th percentile performances, the average file downloading times of feedback-aided retransmission and legacy scheme are 383.8 periods and 481.4 periods, i.e., for D2D Rxs in the 20th percentile, the file downloading time can be reduced by about 100 periods with the feedback-aided retransmission.

2.7 Summary

We proposed a feedback mechanism for LTE-based D2D communication. The proposed feedback mechanism efficiently uses radio resources by allowing multiple D2D Rxs to use one RB at the same time without requiring extra signaling for feedback scheduling. On top of the proposed feedback mechanism, we propose FaRRA algorithm, a rate adaptation algorithm considering the impact of in-band emission. We also propose feedback-aided retransmission method on the proposed feedback mechanism. Through simulations, we evaluate the impacts of near-far problem to the proposed feedback channel and demonstrate that the near-far problem is greatly mitigated by applying OLPC. We find that FaRRA algorithm is robust to in-band emission and uses radio resources more efficiently than the legacy schemes while keeping TBLER under the threshold. We also observe that feedback-aided retransmission improves goodput performances of D2D Rxs with lower 20% performance and shortens file downloading time.

Chapter 3

CoCo: Context aware congestion control scheme for C-V2X communications

3.1 Introduction

According to World Health Organization (WHO), nearly 1.35 million people die in road crashes each year [51]. Autonomous driving technology is one of the candidate solutions to alleviate this problem. Currently, most autonomous driving technologies depend on sensors installed in a vehicle such as Light Detection And Ranging (LiDAR), radar, and cameras. The performances of the sensors are good but significantly affected by environments, e.g., illumination intensity, weather changes, and Non Line of Sight (NLOS) conditions. Therefore, current autonomous driving technology requires constant assistance from the driver.

In recent years, along with the development of communication technologies such as the emergence of 5G and vehicular communications, higher levels of autonomous driving have attracted much attention. Vehicular communications operate independently of the weather, providing better robustness under NLOS conditions compared to sensor-based communications. Vehicular communications can compensate for the limitations of current autonomous driving, leading to realization of higher levels of

Table 3.1: Safety messages in ETSI standard.

Safety messages	CAM	DENM
Traffic type	Periodic	Event-driven
Objective	Recognize surrounding vehicles	Notify detected events
Information	Vehicle status, e.g., location, speed, etc.	Event status, e.g., event identity, location, detected time, etc.
Relay	No relay	One-hop relay

autonomous driving.

Among vehicular communications, Cellular-based Vehicle-to-Vehicle communication (C-V2V) has recently received much attention. C-V2V first appeared in 3GPP Release 14 [52], and it is mostly based on LTE Device-to-Device communication. Therefore, it enables direct communications between User Equipments (UEs) without going through the base station. In autonomous driving, a goal of C-V2V is to recognize surrounding road environments that sensors cannot recognize [53].

To achieve this goal, ETSI defines safety-related messages: Cooperative Awareness Message (CAM) and Decentralized Environmental Notification Message (DENM), which are shown in Table 3.1. Each UE periodically generates and transmits a CAM that contains its own status information such as location, speed, direction, etc. Upon receiving CAMs, a UE can recognize and track other UEs that transmit their CAMs. DENM traffic is caused by events. Therefore, a UE generates a DENM only when it recognizes an event.

ETSI also defines relevance area, which refers to the local area that an event can affect. Thus, DENM traffic allows one-hop relay to disseminate a DENM to UEs in the relevance area. Although C-V2V can complement the limitations of the sensors via the above two types of safety traffic, radio resource congestion problems can limit the performance of C-V2V. There are several reasons why the congestion problem occurs frequently.

Firstly, there is a scarcity of wireless bandwidth in C-V2V. Intelligent Transport System (ITS) band, which is a 5.9 GHz band, is dedicated to vehicular communications and consists of seven 10 MHz channels. Most countries consider allocating two channels for C-V2V [54, 55]. Considering not only V2V but also Vehicle-to-Infrastructure (V2I) and Vehicle-to-Pedestrian (V2P) operations over the two allocated channels, the bandwidth is not enough.

Secondly, different from CAM traffic, which does not take into account relay operation, DENM traffic allows one-hop relay [56, 57]. Therefore, when DENM traffic is generated, the radio resource congestion problem can be more severe due to DENM relaying at receivers. In addition, multiple source UEs can be generated for a single event, i.e., it is possible that multiple source UEs generate redundant DENMs and cause congestion problems.

DENM and CAM traffic have different purposes and generation rules of messages, so applying the same solution to a different kind of these messages is not effective. Hence, considering the characteristics of each safety message, we propose a context-aware congestion control scheme, termed CoCo, that consists of two algorithms for each safety message.

Since a CAM contains a UE's status, the UE can decide whether to postpone or give up its transmission considering its rate of the status change, e.g., the change of its location. Thus, the first algorithm controls the transmission interval of CAM by checking whether the current interval results in redundant CAMs, with respect to channel status and surrounding recognition. In case of DENM traffic, multiple source UEs and relay UEs can occur for an single event. In other words, it is possible to exacerbate congestion problems by generating redundant DENMs. In the second algorithm, UEs decide whether to transmit a DENM according to their location and direction of movement.

The main contributions of this paper are as follows:

- Considering the characteristics of two safety messages, we propose a distributed congestion control scheme, called CoCo, that consists of two algorithm for each safety message and minimizes the performance degradation of CAM and DENM

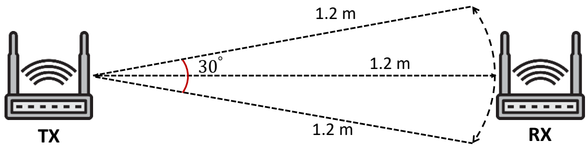

(a) RSS measurement topology

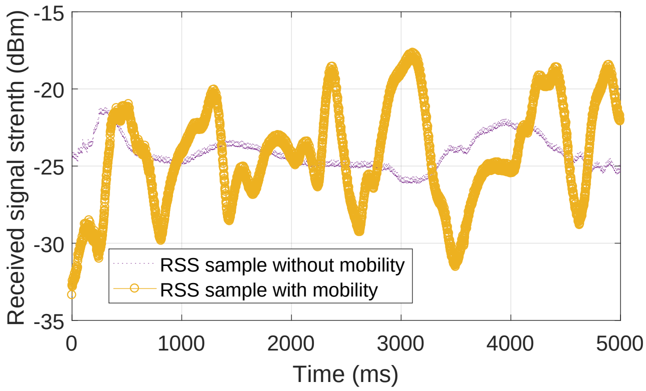

(b) RSS measurement result

Figure 3.1: RSS measurements.

traffic when congestion problems occur in C-V2X communications.

- The proposed scheme is a very feasible solution to mitigate congestion problems because it does not require hardware modification or any signal exchange. More importantly, it is standard compliant.

- We evaluate performance of the proposed scheme via simulation which reflects realistic vehicle mobility and road situations based on Simulation of Urban MObility (SUMO) [31].

3.2 Background

3.2.1 Preliminaries

3.2.2 Fluctuations of Channel Load Measurements

Performance of congestion control schemes in the related work mainly relies on channel load measurements. In a distributed system, each UE performs channel load measurements by comparing the level of RSS with a pre-defined threshold. The channel load measurements are helpful for inferring channel status. However, since the RSS fluctuates quickly, it is difficult to always trust the measurement results. To observe how severe the fluctuations are, we measure RSS samples using USRP-2943.

We use two USRP-2943 devices wired to host PC and set each device as transmitter (TX) and receiver (RX), respectively. As shown in Fig. 3.1a, we fix the position of the TX, and let the RX reciprocate twice for five seconds along the dotted line, keeping the distance to the TX. The transmission power is -7.5 dBm and the carrier frequency is 5.9 GHz, which is ITS band. The interval of RSS samples is 1 ms, which is equal to LTE Transmission Time Interval (TTI).

As shown in Fig. 3.1b, the measurement results with mobility show a severe fluctuation, which has 14 dB difference between 3000 and 3500 ms. In real driving situations, dynamic changes occur more frequently than in the above simple topology. Therefore, the solutions based on only channel load measurements are not reliable. In this paper, we propose a congestion control scheme that uses not only CBR measurements, but also the information obtained from CAM reception to compensate for fluctuations in CBR measurements.

3.2.3 The Current State of ITS Band Plan

In the early stage of ITS band plan, most countries considered that DSRC uses the entire ITS band because there was no competing technology against DSRC. However, with the advent of C-V2V, they have revised their ITS band plan. As shown in Fig. 3.2,

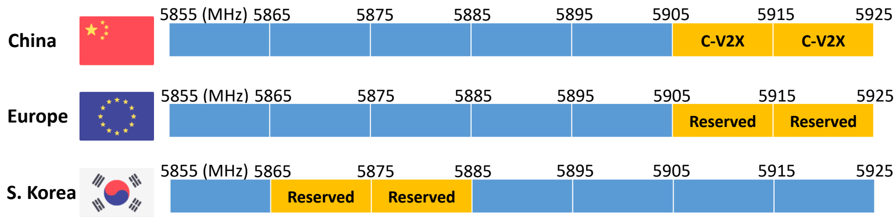

Figure 3.2: ITS spectrum plan.

in the case of China and South Korea, there is a movement to use two channels in the ITS band for C-V2V [54]. Europe maintains technology neutrality between DSRC and C-V2V, and uses two channels in the ITS band for C-V2V trials [55]. Through allocated channels, mobile network operators perform V2I, V2P, and V2V.

Since the US government has indefinitely postponed the policy of mandatory installation of DSRC on all newly produced vehicles, there is a possibility that C-V2V uses the ITS band with DSRC in the US. Therefore, in most countries, two channels in the ITS band will be allocated for C-V2V. Hence, the radio congestion problem can frequently occur in C-V2V because the bandwidth for C-V2V is not sufficient.

Given the latest ITS band plans of each country, it may not be possible for one kind of data traffic to use one channel exclusively, due to its insufficient bandwidth. In this paper, we consider that CAM and DENM traffic share a channel.

3.2.4 Impact on PDR performance caused by DENM

As mentioned in Section **??**, DENM traffic allows one-hop relay. Hence, the resource congestion problem can be more severe due to DENM relaying. In order to investigate the effect of DENM on Packet Delivery Ratio (PDR) performance, we conduct with the number of UEs 250, 500, and 750 in Manhattan grid topology [58] [1] by changing the number of events. Fig. 3.3 shows the simulation results. In the absence of an event, the 750-UE case has the worst performance because the resource congestion level is

[1]The size of Manhattan grid is $1299m \times 750m$ and 500-UE case is the case of sparse density in the Manhattan grid according to [58]

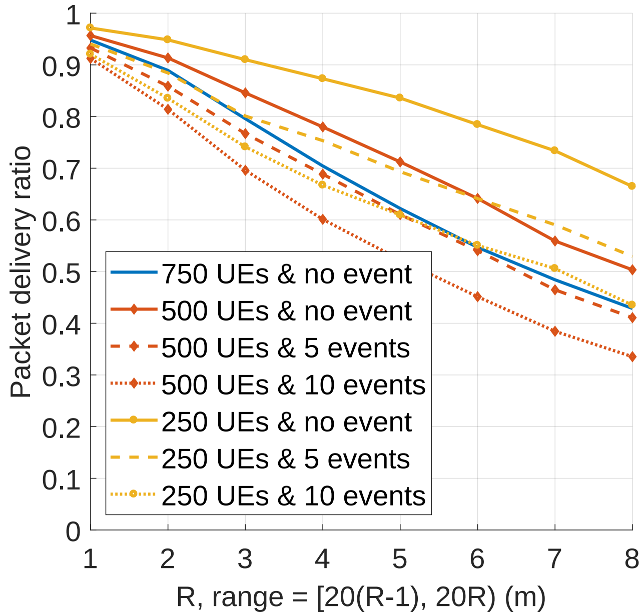

Figure 3.3: Impacts on PDR performance caused by DENM.

the highest. However, in the case of 500-UE, even if the number of events is 5, we confirm that the performance degradation occurs as much as the number of UE is 750.

Since DENM includes many use cases according to the related standard [57], e.g., road hazard warning, traffic signal detection, traffic jam detection, and precipitation, UEs can generate many DENMs frequently on the road. Therefore, it should be taken into account that DENM can exacerbate the resource congestion problem in V2X communication.

3.2.5 Resource Allocation in C-V2V

According to the 3GPP standard [52], C-V2V has two resource allocation modes: centralized mode and distributed mode. Focusing on a distributed communication scenario where vehicles communicate with each other directly, we explain the distributed resource selection mode. First, each UE creates a candidate resource list from the resource pool based on the energy level sensing results measured in the past. Please note that a resource can contain a single message. Thus, the size of the resource in frequency depends on the size of message, and the length of the resource is 1 ms because LTE TTI is 1 ms. For list creation, the UE first excludes from consideration the resources reserved upon CAM reception. Since a CAM contains reservation information of used resources, the UE can learn the reserved resources. Then, the UE adds resources with energy levels below a predefined energy level threshold till resources in the list reach 20% of the resource pool.

Until resources in the candidate resource list occupy 20% of the resource pool, each UE repeats the above process decreasing the pre-defined threshold. The UE then randomly choose a resource from the candidate resource list. In the case of safety-related data traffic, the UE generates and transmits safety-related messages periodically. According to the standards [57], if a UE recognizes an event, it periodically generates and transmits a DENM until the event terminates. Otherwise, the UE does not generate a DENM.

Therefore, C-V2V supports Semi-Persistent Scheduling (SPS) that uses selected resources for a certain period of time to enhance the efficiency of resource allocation. A UE randomly selects a reservation count in the range [5, 15], which refers to the period which unit is the number of transmissions and during which the UE uses the selected resource. Thus, if the UE selects a reservation count, it uses the selected resource for the reservation count and runs scheduling again when the reservation count reaches zero.

3.2.6 Related work

There are several related studies. To the best of our knowledge, there are very few congestion control schemes for C-V2V. However, there are related studies for Dedicated Short Range Communication (DSRC) which is IEEE 802.11p based vehicular communication. Therefore, we conducted more research on DSRC studies to learn trends in congestion control schemes and to find appropriate comparison schemes.

As far as we have surveyed, relevant studies mainly depend on channel load measurements or Channel Busy Ratio (CBR) [10–20]. They adjust transmission parameters such as transmission interval, transmission power, and data rate, based on channel load measurements (or CBR). For example, if the channel load is greater than a pre-defined threshold, the UE increases its transmission interval to reduce the channel load.

However, since channel load measurements fluctuate very much, channel load measurement based solutions are not reliable. In vehicular communication environments, channel load fluctuations become greater with higher mobility. To show how the channel measurement is affected by high mobility, we measure real Received Signal Strength (RSS) samples by comparing the cases with and without mobility. We present the details about the result of the channel measurement in Section 3.2.1.

There are other studies [21–23], which use context information such as UE's location and speed. The study in [21] is application-limited, i.e., lane change. In this study, when the UE attempts to change a lane, it reduces transmission power since it should only communicate with the UEs closest to the UE behind. This study does not apply to controlling the transmission parameters of CAM or DENM, which must be shared with all neighboring UEs. The authors in [22, 23] use context for mitigating the congestion problem.

However, the study in [22] uses strict assumptions and does not comply with the C-V2V standard. In [22], the authors assume that UEs learn the locations of all neighbors as well as transmission probabilities of all potential interferers. A UE can learn the location of a neighbor UE when receiving a CAM, but to know the location of every neighbor, the UE must receive a CAM from each neighbor. This assumption is infeasible. Currently, there is no protocol or procedures to learn transmission probabilities of potential interferers in the standard. The limitations in [23] are the same as those in [22].

We survey the related standard. 3GPP does not propose a specific congestion control mechanism but presents a methodology for congestion control [52]. 3GPP provides two metrics for the congestion control: CBR and Channel occupancy Ratio (CR). CBR refers to the ratio of the subchannels over which the measured Received Signal Strength Indicator (RSSI) exceeds a pre-defined threshold during a measurement window to total subchannels. CR refers to the ratio of subchannels used for transmissions. That is, it is an indication of channel utilization for a UE. The channel utilization refers to the ratio of used resources to total resources during a measurement window.

According to the methodology presented by 3GPP, each UE has a mapping table from CBR to CR. The procedures are as follows. The UE first measures CBR, and maps the CBR to CR and then control transmission interval (or opportunity) based on the CR. The ETSI standard specifies that the CAM transmission interval should be between 100 to 1000 ms. The Modulation and Coding Scheme (MCS) with QPSK and code rate 1/2 is a viable choice for achieving good performance in vehicular communications [59]. Considering this MCS, the number of subchannels in one subframe, i.e., 1 ms, is three.

Thus, Converting the transmission interval to the channel utilization, the channel utilization of CAM ranges from 0.0003 to 0.003. However, CR values specified in the standard [60] range from 0.002 to 0.03. Therefore, it is difficult to apply this method immediately to solving the congestion problem because the CR range does not match the channel utilization range of CAM traffic.

To sum up, the related standards are still lacking consideration of the congestion control mechanism, and the related studies with the context information are less practical due to the strict assumptions and the lack of careful consideration of the related standards. Channel load measurement based solutions may not be effective in mobile environments, but they are feasible in the related standards. Since we propose a feasible solution that complies with the relevant standards, we choose a comparison scheme, taking into account the feasibility for fair evaluation.

The comparison scheme is LIMERIC [20]. LIMERIC is one of the most popular congestion control schemes. Until recently, papers that evaluate performances of

LIMERIC have been published [12, 13]. LIMERIC adapts the transmission rate that is defined as the ratio between resources used for transmission to total resources according to CBR measurements. LIMERIC adjusts the transmission rate R_k every θ as follows.

$$R_k(t) = (1 - \alpha) \times R_k(t - \theta) + \beta \times (CBR_T - CBR_k(t - \theta)), \tag{3.1}$$

where α is a forgetting factor, $CBR_k(t)$ is the channel load measurement of UE k at time t, and CBR_T is a predefined CBR threshold. The larger α, the less the previous R_k is reflected when updating R_k, and β determines how much CBR_k reflects the transmission rate update.

We have also surveyed relaying schemes in vehicular communications. In a broadcast manner, when a UE transmit a message, all RXs can relay the received message. Not only are there too many duplicate relay messages in this situation, there is a possibility that many relay messages will collide. Thus, there have been many efforts to solve the relay problem. There are two representative methods to control the number of relay UEs.

The first method is farthest-first relaying, which assigns a shorter waiting time to a relay UE with a longer distance from the original TX [61–63]. In [63], the proposed scheme exploits directional antennas for efficient relaying. We focus on the scenario that UEs are equipped with an omni-directional antenna rather than a directional antenna. Thus, we consider the farthest-first relaying method with omni-directional antenna as a comparison scheme.

The second method is probabilistic-based relaying, which prevents the relay problem by relaying stochastically to control the number of relay UEs [64–67]. In [67], the authors propose PVCast. PVCast scores packets based on spatial and temporal information and then maps the score to the relay probability (0.3, 0.4, and 0.5). We also use PVCast as a comparison scheme to compare with our proposed algorithm.

3.3 Proposed context-aware congestion control

Considering the charactecristics of two safety messages, we propose a distributed context-aware congestion control scheme, named CoCo, that consists of two algorithms for each safety message, i.e., CoCo-CAM and CoCo-DENM. In this section, we provide the detailed explanation of CoCo.

3.3.1 The design of CAM transmission interval control algorithm

In this subsection, we explain CoCo-CAM algorithm. The key to solving the radio resource congestion problem caused by CAM traffic is whether UEs are enabled to delay or abandon their transmissions to alleviate the congestion level. To this end, we allow each UE to adjust the transmission interval of CAM generation, according to its status change rate, i.e., the change of its location. We consider a distributed system. Each UE generates a CAM periodically, enabled to exploit the information of CAMs received from its neighbors. A CAM consists of status information of the TX such as speed, location, etc. Thus, through CAM reception from neighboring UEs, a UE compares its speed with the speed of each neighbor recognized, and learns how fast it is relatively. Reflecting the current situation, each UE adjusts its transmission interval of CAM.

Algorithm 3 shows the pseudo code of CoCo-CAM, which controls CAM transmission interval. We assume that each UE learns system values such as a Channel Busy Ratio (CBR) threshold (CBR_T), β, and a default channel utilization ratio (R_{ch}^{def}) when receiving service authorization from the mobile network operator. Each UE measures its CBR (CBR_k) at every period. CBR_k is the measured ratio of RSS values greater than the RSS threshold among all sub-channels during the measurement window. β is a parameter that determines how much to reflect the measured CBR_k when updating the channel utilization ratio, R_{ch}^k. The channel utilization ratio, R_{ch}^k, is the ratio of resources used for transmission to total resources in the resource pool. For example, in the case of 100 ms transmission interval, the channel utilization ratio is 1/300. [2] UEs can recognize status information of neighboring UEs from CAM reception and periodically measures CBR. First, UEs create a set of neighbors' speed information, $\boldsymbol{V_k}$. All UEs use this set as core information to control the transmission interval of CAM in CoCo-CAM because the UEs compare their speed with the speed of neighbors to determine the transmission interval of CAM. Before the UE k starts resource selection, it updates $\boldsymbol{V_k}$ from CAM reception (lines 1–3).

The UE k considers its speed first when making the decision on the transmission interval. If the UE k's speed is zero, it postpones resource scheduling by 100 ms (lines 4–6). [3] Since the UE k's status remains the same, the UE k postpones its resource scheduling rather than transmitting a redundant CAM. For non zero speed, the UE k updates R_{ch}^{k} according to CBR_k (line 8). Since the measured CBR_k can vary greatly, we use the minimum function to reflect the current measurement conservatively.

If $|\boldsymbol{V_k}|$ is greater than one, the UE k uses the median of $\boldsymbol{V_k}$. This is because if the UE k uses the mean of $\boldsymbol{V_k}$, too large (or too small) an element value in $\boldsymbol{V_k}$ may result in a biased average. Using the median of $\boldsymbol{V_k}$ results in the unbiased transmission interval of CAM. The UE k finally updates R_{ch}^{k} by multiplying previous R_{ch}^{k} by the weighting factor $\frac{v_k}{v_{median}}$ (line 9–11). Then we convert R_{ch}^{k} to I_k, taking into account that I_k is 100 ms when R_{ch}^{k} is 1/300 (line 13).

The UE k checks whether the obtained final I_k is within the range of CAM generation interval, i.e., $100\ ms \leq I_k \leq 1000\ ms$. If I_k is outside the range, I_k is set to the maximum or minimum value (lines 14–17). Lastly, the UE k initializes $\boldsymbol{V_k}$ to $\emptyset$ for selecting the next transmission interval (line 19).

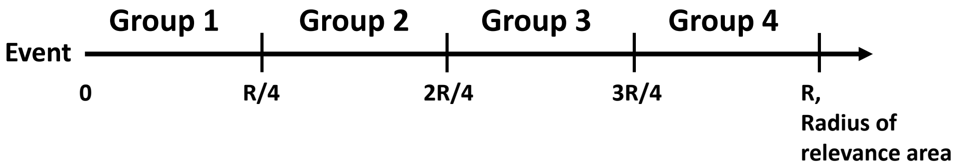

Figure 3.4: Event grouping according to the radius of the relevance area.

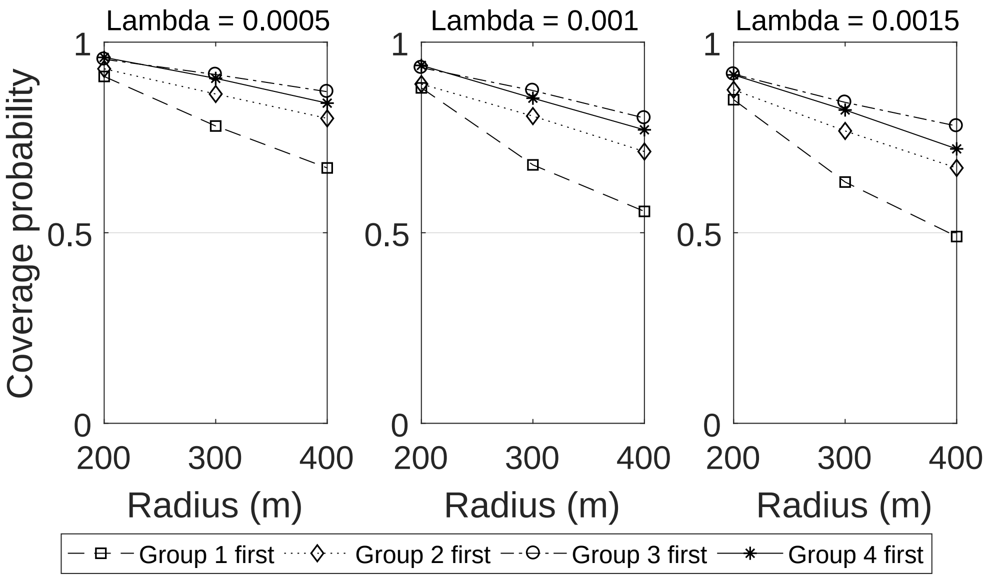

Figure 3.5: Coverage probability when relaying in each group.

3.3.2 The design of DENM transmission control algorithm

In this subsection, we explain CoCo-DENM. The related standard [57] allows DENM to one-hop relay. A single DENM can generate multiple relay UEs. In addition, multiple source UEs can occur with respect to a single event. Therefore, it is important not only to reduce the number of relay UEs, but also to effectively reduce the number of source UEs.

Algorithm 4 shows the pseudo code of CoCo-DENM, which enables UEs to decide

[2]Three subchannels are available for CAM transmission, so there are 300 resources (each with 1 ms transmission time) in total for 100 ms.

[3]According to the standards [56], 100 ms is the minimum value of the CAM generation interval.

whether to schedule and transmit a DENM according to their location and direction of movement. We assume that each UE learns system values such as a resource pool for UEs approaching an event, r^{in}, and a resource pool for UEs moving away from the event, r^{out}, when receiving service authorization from the mobile network operator. CoCo-DENM consists of two parts according to the UE's state, e.g.,source UE or relay UE. The source UE refers to the UE witnessing the event and the relay UE refers to the UE that cannot witness the event, but receives DENM of the event. Please note that UEs cannot be of both types at the same time.

In case of the source UE part (lines 1–18), source UEs themselves judge whether they are moving away from or getting closer to the event i. D_i^k refers to the direction of UE k for event i, i.e., if UE k is getting closer to event i, UE k sets D_i^k to one. In the opposite case, UE k sets D_i^k to zero. We give scheduling priority to UEs getting closer to the event. Since the UEs have a longer lifetime as sources than the UEs moving away from the event and the UEs are directly related to the event, it is reasonable to give the UEs scheduling priority.

If D_i^k is one, UE k selects a resource among r_i^{in}. UE k does not immediately selects a resource through SPS, but first allocates a resource through single TX scheduling (line 3). If UE k immediately selects a resource via SPS and a resource collision occurs, the resource collision can cause severe damage, e.g., failure of message reception, until one resource reservation is terminated. Therefore, in order to reduce the damage, we design to do SPS after single TX scheduling. If UE k receives the same DENM before its TX, UE k cancels its scheduling (lines 5–8).

If UE k does not receive the same DENM after single TX scheduling, UE k selects a resource through SPS (line 10). UE k cancels its scheduling as well, if the UE k receives the same DENM after SPS (lines 12–14). In the case of the UE moving away from the event, the process is the same as above except that the resource pool is changed r_i^{in} to r_i^{out}.

Purpose of the relay is to allow UEs in the relevance area that have not received a DENM to receive the DENM. Like source case, the UEs are more likely to fail to receive the DENM due to resource collisions when all relay UEs relay the same DENM. Therefore, it is important to effectively reduce the number of UEs relaying the same DENM. We design to control the number of relay UEs by grouping them based on the radius of the relevance area as shown in Fig. 3.4. Then, we assign scheduling priorities by different waiting times for each group. The waiting time is set to a multiple of one-fourth of the remaining life time of DENM. To assing the scheduling priority, we analyze coverage probability, P_{cover},based on stochastic geometry [68–70]. The coverage probability means the probability that SINR is higher than the threshold.

$$P_{cover} = \mathbb{P}[SINR > SINR_{Threshold}], \tag{3.2}$$

First, we uses a rectangle Boolean scheme in [69] to model a blockage effect. The scheme follows that $P_{LOS} = exp(-kR)$, where k is an average size of blockages and R is a distance between TX and RX. Given the distance R, we compute its path loss gain $L(R)$ as

$$L(R) = \mathbb{I}(P_{LOS})R^{-p_L} + (1 - \mathbb{I}(P_{LOS}))R^{-p_N}, \tag{3.3}$$

where $\mathbb{I}(\cdot)$ is a Bernoulli variable and p_L and p_N are the LOS and NLOS path loss exponents. We also use Nakagami fading in order to model small-scale fading, h_l. Let N be the thermal noise and P_t is the transmission power. Based on the above assumptions, SINR by UEs with link distance R is expressed by

$$SINR = \frac{hP_tL(R)}{N + I_R}, \tag{3.4}$$

where

$$I_R = \sum h_kP_tL(R_k), \tag{3.5}$$

$L(R_k)$ refers to a path loss gain of interference link distance, R_k. I_R is the cumulative interference from all UEs that select the same resource. Under the assumptions, we distribute UEs according to 2-D Poission point process and observe P_{cover} by changing the density of UEs, $lambda$. In case of $lambda = 0.0005$, on average, 500 UEs are distributed to the area. We use the blockage model and channel model in [69]. We observe the coverage probability when relaying in each group. As shown in the Fig. 3.5, when relaying in group 3, the coverage probability is highest in all environments. Thus, we decide the scheduling priority order in the order of group 3, group 4, group 2, and group 1 based on the coverage probability results.

The UE k identifies the group it belongs to according to its location (line 19). The UE k waits for T_i^l according to the group to which it belongs. Then, the UE k selects a resource for relay. If the UE k hears the same relay DENM before its relay via UE n, the UE k checks the road segment ID of UE n. So, if the road segment ID is the same as that of the UE k, the UE k cancels its relay scheduling. In the opposite case, in order to improve performance in NLOS situations, even if the UE k receives the same relay, the UE k does not cancel its relay.

3.3.3 Properties of CoCo

In a distributed communication system, since each UE has limited information, it often needs more information to make better decisions. However, in case of congestion problems, additional signaling can make the congestion problems worse. In addition, the related standards may need to be modified to transmit the additional signals.

CoCo does not incur additional signaling. Under CoCo-CAM, UEs adjusts the transmission interval of CAM using only the information through CAM reception and CBR measurement results. In like manner, in case of CoCo-DENM, UEs decide whether to schedule and transmit a DENM using only the information through DENM reception (or detection of an event). That is, CoCo does not require any standard or hardware modifications. Thus, CoCo is very effective and practical solution to mitigate congestion problems in a distributed manner.

Table 3.2: Simulation environments.

Carrier frequency	5.9 GHz
System bandwidth	10 MHz (50 RBs)
Topology	Manhattan grid [71]
Number of total UEs	500
Number of events	15
Vehicle mobility model	SUMO [31]
Link performance model	LTE error model [72]H
Channel model	Fast fading + shadowing + pathloss + in-band emission [71]
Modulation	QPSK
Code rate	0.529
TX power	23 dBml
Noise figure	9 dB
CAM size	300 bytes
DENM size	800 bytes
Radius of relevance area	200, 300, and 400 m
Simulation time	100,000 subframes (100 s)

3.4 Performance evaluation

In this section, we evaluate the performance of CoCo (CoCo-CAM and CoCo-DENM) by comparing with the comparison schemes through simulation, which reflects realistic vehicle mobility and road environments in an urban scenario. We assume that CAMs and DENMs are transmitted on the same channel due to insufficient bandwidth. Each UE transmits a CAM according to its CAM transmission interval and transmits a DENM when it recognize an event. DENM relay is attempted if RX is in the relevance area. When evaluating the performance of CoCo-CAM, we conduct performance evaluations without applying DENM algorithm to better understand the effects of CAM algorithms on performance.

In order to fairly evaluate CoCo-CAM, we use two comparison schemes: the legacy scheme and LIMERIC mentioned in Section 3.2.6. LIMERIC adopts CAM transmission interval based on the channel busy ratio measurements. The legacy scheme represents the current 3GPP standard operation that has no congestion control function.

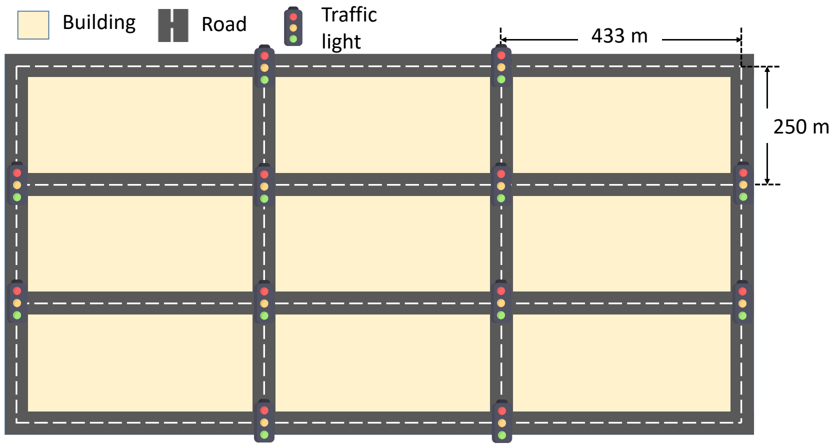

Figure 3.6: Manhattan grid.

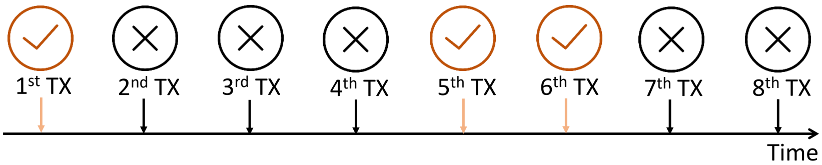

Figure 3.7: Example of reception result for periodic transmission.

CoCo uses the β parameter that helps to determine how much to reflect measured CBR results. The goal of using β in CoCo is the same as that in LIMERIC. Thus, following LIMERIC, we set β as 1/150.

When evaluating CoCo-DENM, we fix the algorithm, which has the best performance among the CAM algorithms beforehand, and then evaluate the performance of CoCo-DENM by comparing with comparison schemes. We use three comparison schemes to fairly evaluate CoCo-DENM. The first one is the legacy scheme that represents the current 3GPP standard. In the legacy scheme, when a UE recognizes or receives a DENM, the UE always transmits the DENM. The second one is farthest-first method mentioned in Section 3.2.6 and the last one is PVCast, which is likewise mentioned in Section 3.2.6.

3.4.1 Simulation Environments

Table 3.2 shows the parameters for simulation environments.

Topology and mobility model: We consider an urban scenario. The 3GPP recommends using the Manhattan grid topology when evaluating the performance of C-V2V in urban scenarios [71]. Thus, we use the Manhattan grid as the evaluation topology. As shown in Fig. 3.6, the topology includes a total of nine 433 m $\times$ 250 m-sized grids and traffic lights that are installed at each intersection. In the Manhattan grid scenario, the number of UEs that generate medium traffic in [71] is 500. Events are generated according to a uniform distribution, and we conduct performance evaluation with 10 seeds.

Channel model: 3GPP also recommends the channel model for evaluating the performance of C-V2V in urban scenarios [58]. According to the recommendation, we use the WINNER+ B1 model as the pathloss model [50] and the shadowing model which follows log-normal distribution with 3 dB and 4 dB standard deviations for LOS and NLOS conditions, respectively. We also consider fast fading generated by ITU-R IMT UMi model in [49]. Since we use only one channel, there is no Out of Band (OOB) emission, but in-band emission, which is undesired emission to subchannels under the same time resource, exists. Thus, we adopt the model in [48] to generate in-band emission.

Link performance model: We use an established LTE link performance model [72] implemented in ns-3 [73], which is one of the well-known simulators in the field of network and communications. Thus, our simulator uses this model to determine whether message reception is successful or not by mapping SINR to Transport BLock Error Rate (TBLER).

Resource pool: We consider one channel in ITS band, and the bandwidth of the channel is 10 MHz, 50 Resource Blocks (RBs). We also consider using QPSK & code rate of 0.529, which is known to provide good performances in vehicular communi-

Table 3.3: Average transmission interval.

Radius of relevance area	200 m	300 m	400 m
CoCo	197 ms	212 ms	211 ms
LIMERIC	181 ms	232 ms	246 ms

cations [59]. According to the MCS level, 15 RBs forms one subchannel considering CAM size 300 B. Therefore, in the case of CAM, there are 3 $(= \lfloor 50/15 \rfloor)$ subchannels. In the case of DENM, there is 1 $(= \lfloor 50/40 \rfloor)$ subchannel considering DENM size 800 B.

3.4.2 Performance Metrics

Packet delivery ratio: Packet Delivery Ratio (PDR) is a metric that indicates CAM (or DENM) reception ratio of UEs within the range of TX UE. We observe PDR performance by varying the range at 20 m intervals following the methodology of the 3GPP standard [58], i.e., we observe PDR performances at 20 m intervals from 0 m to 160 m.

Shaded distance: The shaded distance is the average distance traveled by TX UE while RX UE is not receiving CAM consecutively. From RX UE's point of view, the goal of CAM is to recognize surrounding UEs. Therefore, it is meaningful to observe the shaded distance metric by observing how CAM reception failure affects the recognition of surrounding UEs.

For example, we assume a simple scenario that there is one pair (TX UE-RX UE), and the TX UE transmits CAM eight times. If RX UE does not hear the second to fourth transmitted CAMs and the seventh and eighth transmitted CAMs as shown Fig. 3.7, the shaded distance is the average distance between the distance traveled by TX UE during three consecutive failures and the distance traveled by TX UE during two consecutive failures.

Distance difference: Shaded distance is a measure of the impact of CAM reception failure on other UEs recognition. The distance difference is a measure of the impact of CAM reception success on other UEs recognition. Thus, the distance difference is the average distance between the distances traveled by TX UE between successfully received CAMs. For example, as shown in Fig. 3.7, the distance difference is the average distance between the distance traveled by TX UE from the first TX to the fifth TX and the distance traveled by TX UE from the fifth transmission to the sixth transmission.

Number of TX UEs: We propose a DENM algorithm that can effectively reduce the number of source and relay UEs. Thus, we also observe average number of TX UEs. Observing with PDR performance, we can see how efficiently each scheme adjusts the number of TX UEs.

3.4.3 Simulation Results

First, we observe the effect of CoCo-CAM on the performances. Fig. 3.8 shows average CAM PDR performances with varying the radius of relevance area. As shown in Fig. 3.8, the first overall trend is that both LIMERIC and CoCo-CAM show better CAM PDR performance than that of the legacy scheme. Besides, we observe that CoCo-CAM gains about 11% performance gain compared to LIMERIC. The main reason for the performance improvements is due to the difference in behavior that LIMERIC schedules and transmits CAM regardless of the state of UE, while CoCo-CAM delays CAM scheduling time when a UE is stationary.

The second overall trend is that the larger the radius of relevance area, the lower the performance of the three schemes. This is because as the radius of relevance area increases, the number of UEs to relay received DENMs increases. The results also show that the larger the radius of relevance area, the smaller the performance difference between CoCo-CAM and LIMERIC. LIMERIC utilizes only CBR measurements while CoCo-CAM utilizes not only CBR measurements but also the information from CAM reception.

Therefore, as shown in Table 3.3, LIMERIC increases the transmission interval more sensitively in case of more significant congestion level. However, CoCo-CAM does not set a long transmission interval like LIMERIC because it selects the transmission interval by using the context information as well. Thus, in terms of the average PDR performance, the larger radius, the smaller the performance gap between CoCo-CAM and LIMERIC. In other words, Since CoCo-CAM's dependence on CBR, like LIMERIC, increases due to reduced CAM reception, CoCo-CAM behaves almost like LIMERIC and opportunistically leverages the information from CAM reception. Therefore, even with very high levels of congestion in radio resources, there is no performance reversal between CoCo-CAM and LIMERIC.

Since the three schemes transmit at different transmission intervals during the simulation, the number of CAM transmitted depends on each scheme. Therefore, a high CAM PDR result does not guarantee that UEs track other UEs well. Thus, we look at the additional metric to see how well the UEs track other UEs through CAM reception.

Fig. 3.9 shows a distance difference performance as the radius of relevance area changes. As shown in Fig. 3.9, we observe that the legacy scheme performs slightly better than the other two schemes. These two schemes can set the transmission interval to a value greater than 100 ms based on CBR and the context information, while the legacy scheme always sets the transmission interval to 100 ms. Thus, the legacy scheme can get slightly better performance when UEs receive CAM well. Also, CoCo-CAM only schedules when there is motion in a UE, but the other two schemes schedule and transmit even when there is no motion. Hence, considering the performance of recognizing UEs with mobility, CoCo-CAM achieves better performances than LIMERIC and the legacy scheme.

As shown in Fig. 3.10, the legacy scheme shows the worst shaded distance performance. It means that poor CAM reception can drastically reduce the tracking accuracy of other UEs. On the other hand, CoCo-CAM shows the best performance compared to the legacy scheme and reduces the average shaded distance by up to 26% compared to that of LIMERIC. This is because CoCo-CAM weights the context information, $\frac{v_k}{v_{median}}$, to update CAM transmission interval and sets a more meaningful transmission interval.

In order to evaluate the performance of CoCo-DENM, we fix the CAM transmission interval algorithm with CoCo-CAM and evaluate CoCo-DENM by comparing with the comparison schemes.

First, we observe average DENM PDR performances as shown in Fig. 3.11a. When the radius of the relevance area is small, the difference in the performance between algorithms is not great. However, as the radius increases, the difference in performance increases, and performance gains of up to 18$\%$ are observed. There are two reasons why CoCo-DENM achieves performance gain.

The first reason is that there are few resource collisions between source UEs compared to other algorithms. In the proposed algorithm, even if a resource collision occurs, the resource collision is resolved in most cases because UEs do SPS after single TX scheduling. However, in the case of other algorithms, UEs do SPS without single TX scheduling. Therefore, Resource collisions continue to cause severe damages until either resource reservation is over.

The second reason is that the proposed algorithm reduces the number of relay UEs more effectively. As shown in Fig. 3.12, in the case of CoCo-DENM, it has a bit more relay UEs that that of farthest algorithm because the proposed algorithm check the road segment ID of the UE that transmit the relay and then cancels its own relay only if the road section is the same in order to enhance the performance of NLOS situations. However, in other comparison schemes, there is no design for NLOS situations.

As shown in Fig. 3.11c, in the legacy scheme, we confirm that the CAM PDR is the lowest becuase all UEs that received DENM transmit the same DENM. However, the proposed algorithm has little effect on CAM PDR performance. Thus, in summary, CoCo-DENM raises DENM PDR performance with little effect on the CAM PDR performance.

3.5 Summary

In this paper, as far as we survey, we first present why the congestion problems can frequently occur in V2V communications. Then, we propose a context-aware congestion control scheme, CoCo, which aims to mitigate the congestion problems and consists of two algorithms (CoCo-CAM and CoCo-DENM) to cope with the congestion problems caused by each message. CoCo also complies with the related standard. Thus, CoCo does not cause additional signals as well as hardware modifications. Through simulations, we show that CoCo-CAM achieves superior CAM PDR performances compared to other comparison schemes and that CoCo-CAM reduces the average shaded distance by up to 26% compared to LIMERIC. We also observe that CoCo-DENM achieves the performance gain up to 20% in terms of DENM PDR performances. In summary, CoCo is very effective and practical solution to mitigate congestion problems in a distributed manner.

Algorithm 3 Transmission interval control in CoCo

Input:

CBR_T {Pre-defined CBR threshold}

CBR_k {CBR measured by UE k}

β {Measurement reflecting parameter}

v_k {Speed of UE k}

$\boldsymbol{V_k}$ {Set of speeds for neighboring UEs recognized by UE k}

T_{sch}^k {Scheduling time of UE k}

R_{ch}^k {Channel utilization ratio of UE k}

R_{ch}^{def} {Default channel utilization ratio}

Output:

I_k {CAM transmission interval of UE k}

When UE k receives CAM transmitted by UE n: $v_n > 0$

1: $\boldsymbol{V_k} \leftarrow \boldsymbol{V_k} \cup v_n$

When UE k starts resource selection: $v_k = 0$

2: $T_{sch}^k \leftarrow$ the current time $+ 100$

3: $R_{ch}^k \leftarrow R_{ch}^{def} + min\{\beta(CBR_T - CBR_k), 0\}$ $|\boldsymbol{V_k}| > 1$

4: $v_{median} \leftarrow median(\boldsymbol{V_k})$

5: $R_{ch}^k \leftarrow R_{ch}^k \times \frac{v_k}{v_{median}}$

6: $I_k \leftarrow \frac{1}{3R_{ch}^k}$ $I_k < 100\,ms$

7: $I_k \leftarrow 100\,ms$ $I_k > 1000\,ms$

8: $I_k \leftarrow 1000\,ms$

9: $\boldsymbol{V_k} \leftarrow \emptyset$

Algorithm 4 DENM transmission control in CoCo

Input:

$\boldsymbol{r_i^{in}}$ {Resource set for UEs entering the event i}

$\boldsymbol{r_i^{out}}$ {Resource set for UEs away from the event i}

$\boldsymbol{r_i^{l}}$ {Resource set for the group l of the event i}

D_i^k {Moving direction of UE k for the event i}

I_i^k {Indication of the first attempt of UE k in resource scheduling}

G_i^k {Group index of UE k for the event i}

T_i^l {Waiting time of group l of the event i}

T_i^k {Reception time of UE k of the event i}

$Road_k$ {Road segment ID where UE k is located}

When UE k is a source UE for the event i: $D_i^k = 1$ $I_i^k = 1$

1: Resource selection among $\boldsymbol{r_i^{in}}$ via single TX scheduling
2: $I_i^k = 0$ Hear the same DENM before its TX
3: Cancellation of its DENM scheduling
4: $I_i^k = 1$
5: Resource selection among $\boldsymbol{r_i^{in}}$ via SPS
6: $I_i^k = 1$ Hear the same DENM before its TX
7: Cancellation of its DENM scheduling
8: The same process as lines 1 to 15 with $\boldsymbol{r_i^{out}}$

When UE k is a relay UE for the event i:

9: Check the group to which UE k belongs Current time $= T_i^k + T_i^l$
10: Resource selection among $\boldsymbol{r_i^{l}}$ via single TX scheduling Hear the same relay DENM before its relay via UE n $Road_k = Road_n$
11: Cancellation of its DENM scheduling

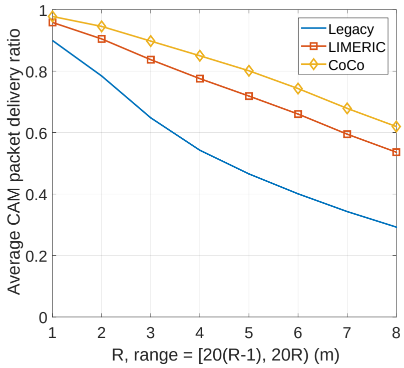

(a) Radius of the relevance area = 200 m

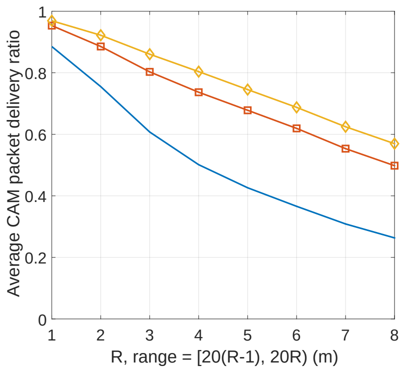

(b) Radius of the relevance area = 300 m

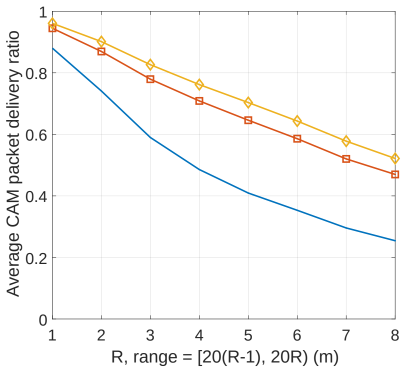

(c) Radius of the relevance area = 400 m

Figure 3.8: CAM PDR performance as the radius of the relevance area changes: (a) 200 m, (b) 300 m, and (c) 400 m.

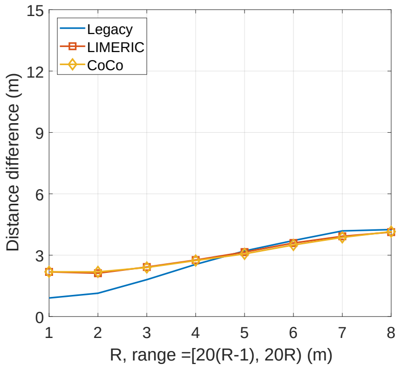

(a) Radius of the relevance area = 200 m

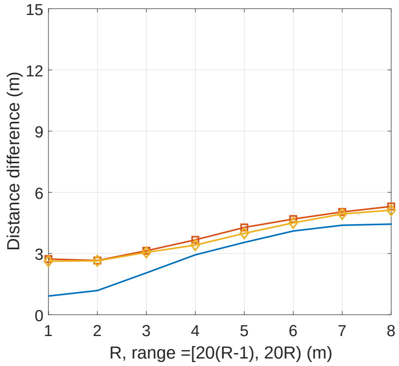

(b) Radius of the relevance area = 300 m

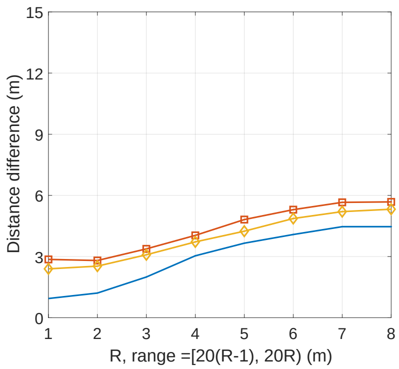

(c) Radius of the relevance area = 400 m

Figure 3.9: Distance difference performance as the radius of the relevance area changes: (a) 200 m, (b) 300 m, and (c) 400 m.

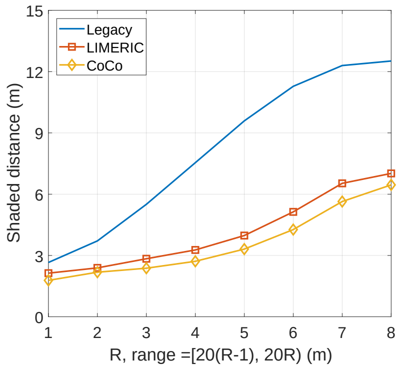

(a) Radius of relevance area = 200 m

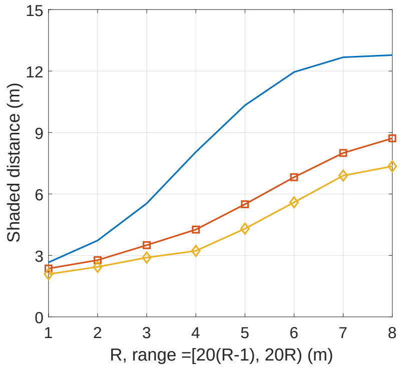

(b) Radius of relevance area = 300 m

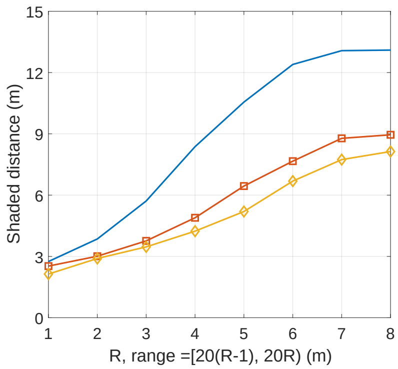

(c) Radius of relevance area = 400 m

Figure 3.10: Shaded distance performance as the radius of relevance area changes: (a) 200 m, (b) 300 m, and (c) 400 m.

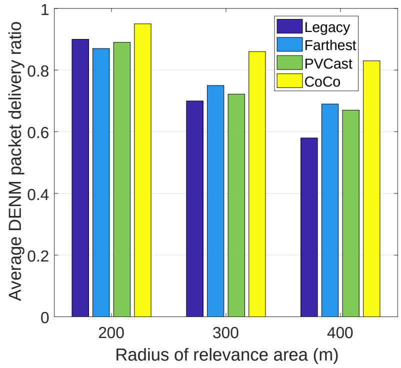

(a) Average DENM PDR

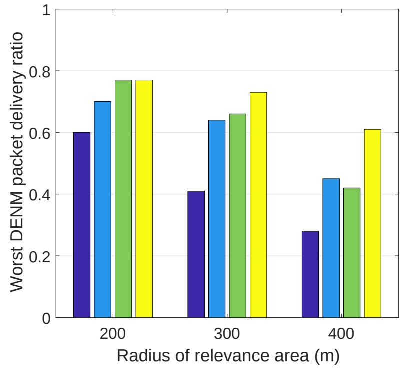

(b) Worst DENM PDR

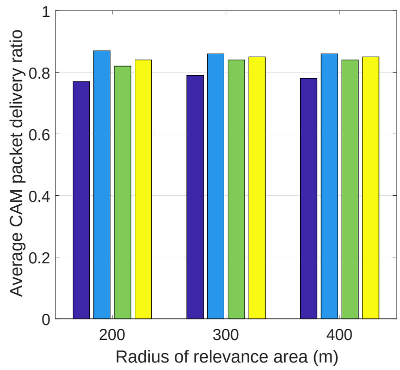

(c) Average CAM PDR

Figure 3.11: PDR performances: (a) average DENM PDR, (b) worst DENM PDR, and (c) average CAM PDR.

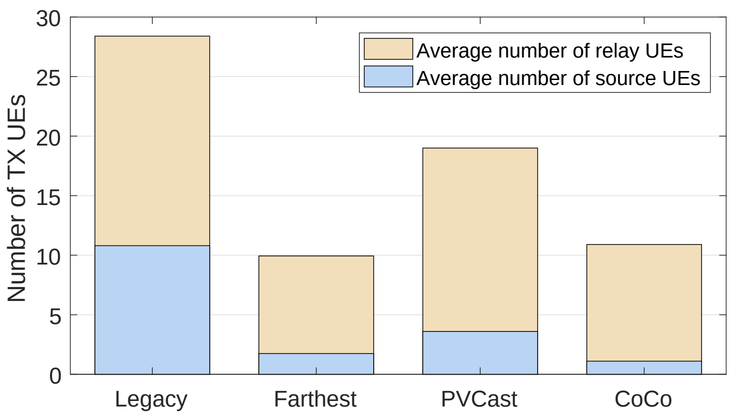

Figure 3.12: Number of TX UEs according to schemes.

Chapter 4

IDC-aware resource allocation based on multi-agents reinforcement learning

4.1 Introduction

Nowadays most smartphones are equipped with several Radio Frequency (RF) modules that these smartphones are able to connect concurrently to multiple heterogeneous networks. These RF modules are located in very close proximity within a single device. Therefore, when these RF modules operate simultaneously at adjacent channels, these RF modules strongly interfere with each other via Out-of-Band (OOB) emission. The damages caused by this interference are called In-Device Coexistence (IDC) problem.

So far, IDC problems have been mainly caused by RF modules between LTE and WLAN, RF modules between LTE and Bluetooth, and LTE and GNSS. However, with the recent development of communication technology, 5G communication has also received a lot of attention between LTE and New Radio (NR) RF modules. The Third Generation Partnership Project (3GPP) is currently in the process of specifying a new fifth generation (5G) communications referred to as New Radio NR. NR has several key features: (i) higher frequency operation and spectrum flexibility, (ii) ultra-lean design, and (iii) forward compatibility.

Since NR was designed with future performance enhancements and application diversification in mind, it is a significant difference from the design of existing LTE systems, e.g., most reference signals used in LTE are not used in NR. As a result, NR does not support backward compatibility with LTE. Thus, 3GPP will standardize the installation of both LTE and NR on a single device to address this backward compatibility issue. As a result, IDC problem can occur in a UE, which is equipped with LTE and NR RF modules.

In the standard [58], NR sidelink also can operate at Intelligent Transport System (ITS) band, i.e., 5.9 GHz band. That is, NR and LTE sidelinks can operate simultaneously on adjacent channels. Hence, currently, 3GPP recognizes the IDC issues in NR UE and propose solutions, i.e., FDM-based solution and TDM-based solution. First, TDM-based solution is free from the IDC problems. However, in the case of sidelink, TDM-based solution is not suitable because main traffic sensitive to delay is considered in a sidelink environments. Second, the FDM solution attempts to alleviate the IDC problem by inserting a guard band between each channel. Since bandwidths for V2X communication are not enough, it is also not appropriate to use guardbands to alleviate the IDC problem.

Our goal is to select clean resources while minimizing the IDC problem when NR UEs select their own resources. RL has received a lot of attentions to address decision making under uncertainty. Through this work, we propose IDC-aware resource allocation based on multi-agents Reinforcement Learning (RL). We claim the following major contributions:

- We model a realistic IDC interference between LTE and NR at ITS band.
- We formulate a IDC-aware resource allocation as a multi-agent reinforcement learning that each UE collects local observations and selects an action and then achieves a reward.
- We confirm that the multi-agents successfully learn their policies and achieves

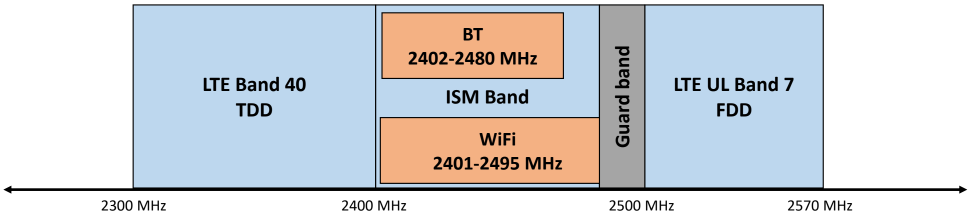

(a) Coexistence of LTE with ISM technologies

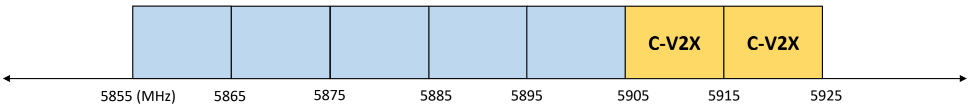

(b) Coexistence of LTE with NR

Figure 4.1: IDC issues.

higher Packet Delivery Ratio (PDR) performances compared to the legacy scheme.

4.2 Background

4.2.1 In-Device Coexistence issues

As shown in Fig. 4.1a, lower portion of ISM band is close to LTE TDD band 40. In case of coexistence between LTE and BT, LTE transmitter causes interference to BT receiver and BT transmitter causes interference to LTE receiver. Similar interference also exists for coexistence case between LTE and Wifi. Figure 4.1a also shows there is 20 MHz seperation between BT and LTE FDD band 7 uplink. Here LTE transmitter causes interference to BT receiver. There is no impact on LTE receiver from BT transmitter because corresponding LTE FDD band 7 downlink is far away from ISM band. Uplink of LTE band 13 (777–787 MHz) and band 14 (788–798 MHz) can disrupt the working of GNSS receiver using L1 frequency (1572.42 MHz). This is the second harmonic of band 13 and second harmonic of band 14 are close to L1 frequency. As shown in Fig. 4.1b, channels for C-V2X are adjacent. Thus, when NR and LTE operate in the ITS band, there is a high probability of using adjacent channels. In that case, LTE (or NR) transmitter causes interference to NR (or LTE) receiver.

4.2.2 In-Device Coexistence scenarios

It is the most popular use case where voice data from LTE is relayed to a BT headset. The voice traffic has to be synchronized on the respective radio interfaces to meet the Quality of Service (QoS) requirement. LTE operation in band 7 and band 40 will cause interruption in service. While downloading High Definition (HD) video on LTE air interface, audio is relayed to BT headset. LTE operationin band 7 and band 40 will cause interruption in service. Lastly, when WiFi coverage is available to a multi radio device, which is enable to use LTE and WiFi, it accesses data on WiFi interface. However, high priority traffic such as an incoming voice call is carried over LTE air interface. Here the WiFi radio operates as a terminal in infrastructure mode. LTE operation in band 7 and band 40 will cause interruption in service.

4.2.3 Related work

Since NR standalone V2V has not been completed, there are no studies dealing with IDC problem between NR and LTE sidelinks. However, there are some studies considering IDC problem between LTE and WLAN [24–26]. There is also a study considering IDC problem between LTE and GNSS [27]. However, All of the above authors consider the resource allocation method of the base station.

We also surveyed multi-agent reinforcement learning-based resource allocation for V2V communication. There are several studies [28–30]. In [28, 29], the authors consider that UEs select resources via multi-agent reinforcement learning. However, they do not consider IDC problem, i.e, they only take into account the interference generated by the same resource selection.

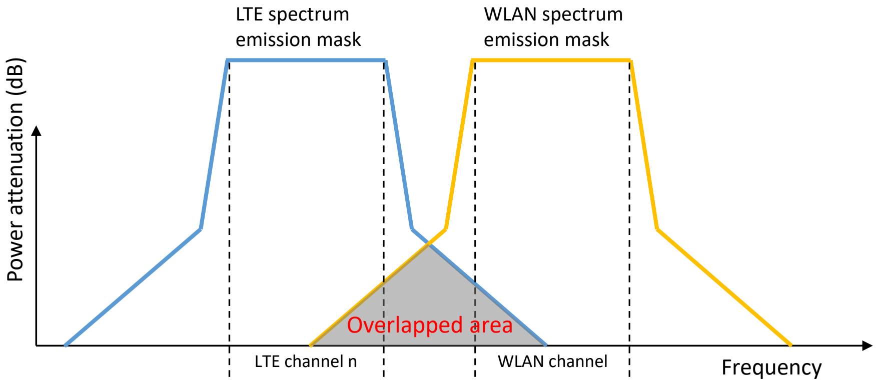

Figure 4.2: IDC interference modeling.

4.3 IDC interference modeling

In order to reflect realistic IDC problems, it is very important to realistically model IDC interference. As far as we surveyed, there is one reference to model IDC interference [26]. The authors [26] model IDC interference that an overlap factor (X) can be used to measure the ratio of the leaked WLAN (or LTE) power at the LTE (or WLAN) receiver to the total WLAN (or LTE) power. Let $S(f - f_n)$ represent the LTE receiver filter transfer function operating at channel n with frequency f_n. Also, let $S'(f - f')$ denote the WLAN power spectral density centered at f', which is approximated by its transmit spectrum mask. Then, the overlap factor of the WLAN and LTE filters of UE k given that the LTE radio is assigned to channel n is expressed as

$$X_{n,k} = \frac{\int S_k(f - f_n)S'_k(f - f')df}{\int S'_k(f - f')df}, \tag{4.1}$$

Then, the IDC interference that affects LTE channel n when it is allocated to UE k is expressed as $I_{n,k} = P \times X_{n,k}$.

However, the IDC interference modeling has some limitations. First, this method provides only fixed IDC interference over an adjacent channel regardless of the locations of selected resources and the amount of the selected resources. As shown in Fig. 4.2, the attenuation of transmission power depends on the locations of selected

Table 4.1: 3GPP spectrum emission mask for ITS band.

f_{oob} (MHz)	10 MHz	Measurement bandwidth
$\pm$ 0-0.5	$-13 - 12\|f_{OOB}\|/MHz$	100 kHz
$\pm$ 0.5-5	$-19 - \frac{16}{9}(\|f_{OOB}\|/MHz - 0.5)$	100 kHz
$\pm$ 5-10	$-27 - 2(\|f_{OOB}\|/MHz - 5.0)$	100 kHz

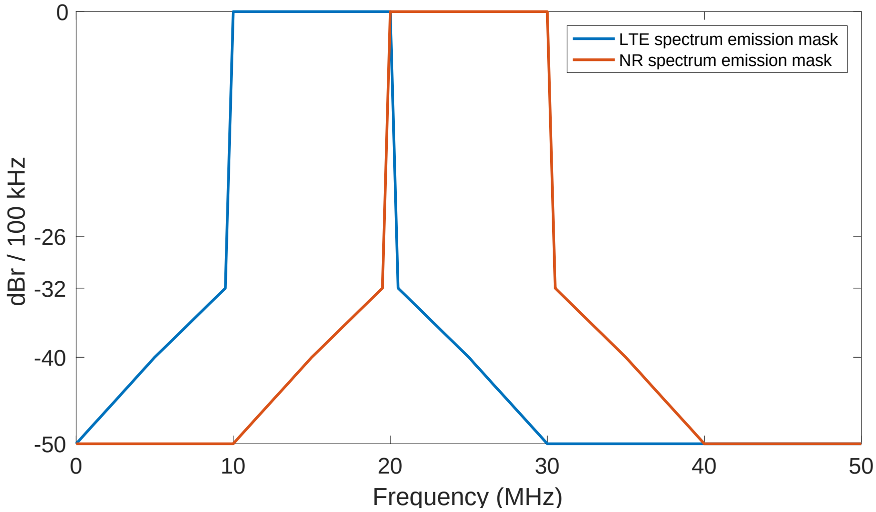

Figure 4.3: Spectrum emission masks for LTE and NR.

resources and the amount of the selected resources.

We model IDC interference based on Table. 4.1. The table 4.1 indicates the amount of the spectrum emission limit according to the location of frequency resources specified at the related standard [74]. Therefore, out method to model IDC interference determines the amount of IDC interference according to the locations of selected resources and the amount of the selected resources. According to the standard [74], spectrum emission mask for NR is the same as the that of LTE as shown in the Fig. 4.3. Thus, the magnitude of IDC interference that each RF module exerts on each other is symmetric.

Figure 4.4 shows the amount of IDC interence varying with the location of selected resources and the amount of the selected resources. We confirm that the amount of IDC interference by our modeling depends on the location of the selected resources

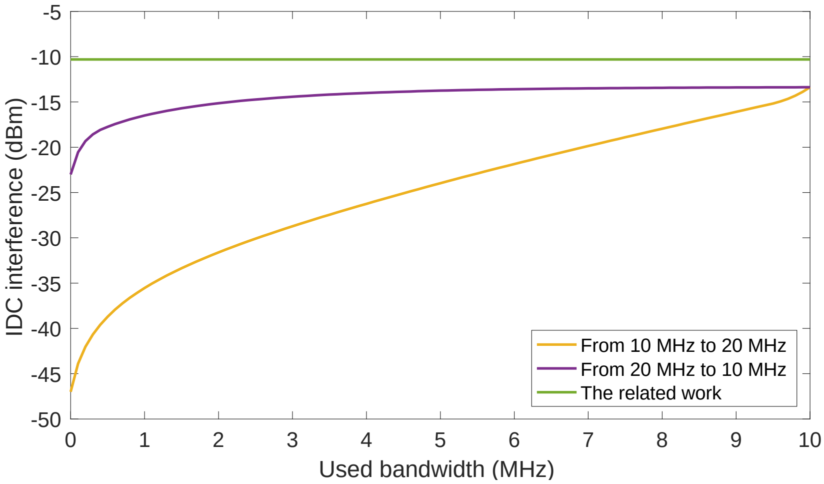

Figure 4.4: IDC interference modeling.

and the amount of the selected resources. As a result, we provide more realistic IDC interference.

4.4 System model

We consider C-V2X communication network in a distributed manner, i.e., UEs communicate directly with each other via sidelink. There are k UEs, which are equipped with NR and LTE RF modules. Through NR and LTE RF modules, each UE transmits periodically packets. Channels for NR and LTE are separate. Thus, UEs can suffer from IDC problems.

Since we focus on a distributed communication scenario, UEs follow mode 4 operation defined in the standard [58]. In mode 4, there is a resource pool of radio resources that all UEs can autonomously select for V2V communication. In our work, each UE selects resources for LTE-V2V communication through mode 4. In case of NR-V2V communication, each UE selects resources for NR-V2V communication via multi-agent reinforcement learning. We assume that NR has the same numerology as LTE, i.e., the subcarrier spacing of NR is 15 kHz.

Orthogonal Frequency Division Multiplexing (OFDM) is exploited to convert the frequency selective wireless channels into multiple parallel flat channels over different subcarriers. Several subcarriers are grouped to form a spectrum subchannel. Since we consider a packet size as 300 bytes and consider QPSK and 1/2 code rate, one subchannel consists of 180 subcarriers (15 RBs). We consider channel fading is the same within one subchannel. Our channel model also assumes that small-scale fading assumed to be exponentially distributed with unit mean and includes path-loss and log-normal shadowing.

4.5 IDC-aware resource allocation based on multi-agent reinforcement learning

Multiple UEs attempt to use radio resources for LTE and NR V2V communications. When each UE selects resources for LTE-V2V communication, the UE selects resources via mode 4. In case of NR-V2V communication, each UE acts as an agent and interacts with the unknown communication environment to achieve experiences that are used to update its own policy. Thus, when each UE selects resources for NR V2V communication, the UE explore the environments and make a decision for resource selection based on its own observations of the environment.

Multi-agent reinforcement learning consists of two phases, i.e., learning phase and test phase. In the learning phase, each UE adjusts its action to maximize its own reward through updating its Deep Q-Network (DQN). In the test phase, each UE observes a local environment and then selects its action based on the local environment and the learned DQN.

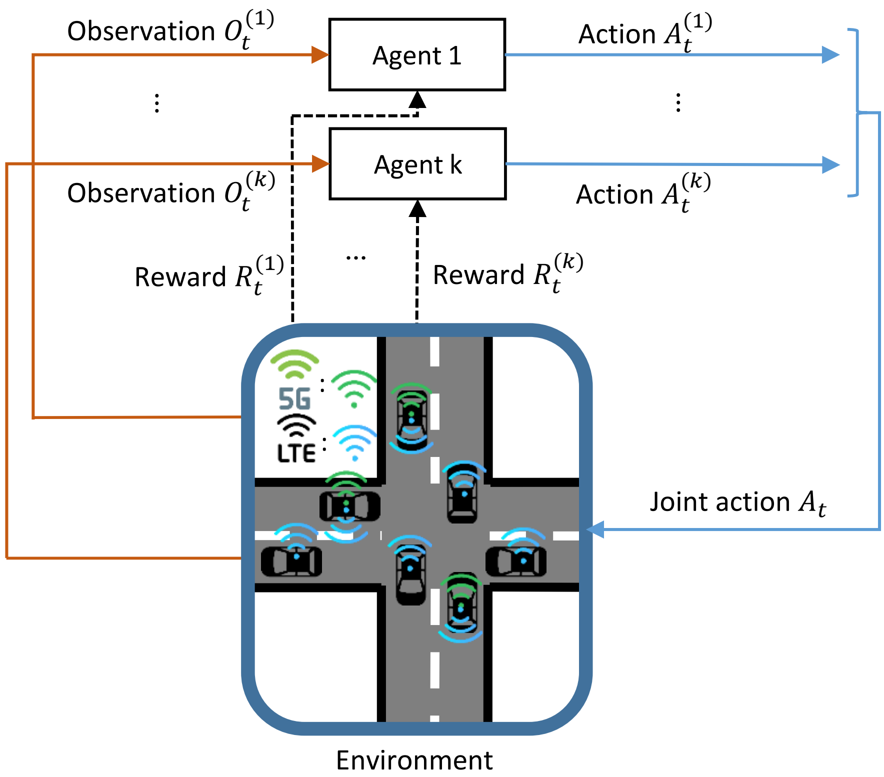

Figure 4.5: Multi-agent reinforcement learning for V2X communications.

4.5.1 Multi-agent reinforcement learning issues

If all agents observe the global environment, then we can model a cooperative multi-agent system as a single meta-agent. However, the size of this meta-agents' action space grows exponentially in the number of agents. Furthermore, it is not applicable when each agent achieves different observations that may not disambiguate the environment, in which case decentralized policies must be learned.

A popular alternative is independent Q-learning (IQL), in which each agent independently learns its own policy. However, IQL introduces a limitation. The weakness of IQL is that, by treating other agents as part of the environment, it ignores the fact that such agents' policies are changing over time, rendering its own Q-function non-stationary. To resolve this problem, agents have to in principle learn a mapping from the weight of other agents'network. Clearly, if the other agents are using deep models, then the other agents' network is far too large to include as input to the Q-function.

In [75], the authors solve the above problem. A key observation is that each agent does not need to be able to condition on any possible other agents' network, but only those values of the other agents' network that actually occur in its experience replay. Thus, they propose a low-dimensional fingerprint that contains this information. Clearly, such a fingerprint must be correlated with the true value of state-action pairs given the other agents' policies. An obvious factor is the learning iteration number, e. Another key factor is the rate of exploration, ϵ. Therefore, we assume that each agent share its own parameters (e and ϵ) with other agents when they receive messages from other agents.

4.5.2 Observation space and action space

Each agent observes a part of the global state every time step t. S_t is the global state at time step t. The local observation consists of two parts. The first part can be obtained by an agent itself. Therefore, the first part includes Received Signal Strength Indicator (RSSI) map of the resource pool measured by itself and its own selected LTE resource information. The second part can be obtained from neighbor. Thus, the second part includes fingerprint information, e and ϵ, and the NR reception indicator of packet transmitted by agent k, R_k^{NR}. Each agent selects an action among action space. The action of an agent is the resource selection for NR. Thus, the action space contains indexes of NR resources.

4.5.3 Reward design

What makes RL appealing for solving problems with hard-to-opimize objectives is the flexibility in its reward design. The system performance can be improved when the designed reward policy at each step correlates with the desired objective.

Our objectives are twofold: maximizing the average PDR of NR and minimizing the damages caused by IDC problem. In order to solve the first objective, we simply consider the summation of NR reception indicator, R_k^{NR}. It can be calculated as,

$$R_{NR} = \sum_{neighbor} R_k^{NR}. \tag{4.2}$$

To address the second objective, we set the penalty reward, $R_{penalty}$, which reflects the damages caused by IDC problem. There are three cases of IDC problem between NR and LTE, i.e., TX-TX, TX-RX, and RX-TX. TX-RX (or RX-TX) scenario cause the worst damage to receiving RF module. In case of TX-TX scenario, the damage depends on the occurrence of resource collision and can be minor when there is no resource collision. Thus, considering the degree of damage, $R_{penalty}$ is determined as,

$$R_{penalty} = \begin{cases} -1 & \text{if TX-RX or RX-TX;} \\ -\frac{1}{neighbor} & \text{if TX-TX.} \end{cases} \tag{4.3}$$

To combine R_{NR} and $R_{penalty}$, we set the total reward at each time step t as,

$$R_t = R_{NR} + R_{penalty}. \tag{4.4}$$

4.5.4 Learning algorithm

We focus on an episodic setting with each episode spanning a period, 100 ms. Each episode starts with random environment state, and lasts until the end of the period. We apply multi-agent reinforcement learning with DQN and add fingerprint method to stabilize experience replay. Each agent has a dedicated DQN that takes as input the local observation at time step t and outputs actions, which is a resource index among the action space.

Algorithm 5 shows the learning procedure. Each agent learns its own DQN through multiple episodes and during learning phase, each agent explores the state-action space with ϵ-algorithm that selects an action via its own policy with probability $1 - \epsilon$ and

Algorithm 5 Learning algorithm of multi-agent reinforcement learning

Initialize Q-network for all agents
for each episode **do**
  for each step t **do**
    for each agent k **do**
      Update locations and channel components
      Observe $O_t^k(S_t)$
      Choose action A_t^k from $O_t^k(S_t)$
      Receive reward R_t^k
    for each agent k **do**
      Observe $O_t^k(S_{t+1})$
      Store $(O_t^k(S_t), O_t^k(S_{t+1}), A_t^k, R_t^k)$ in the experience replay
  if Q-network update episode **then**
    for each agent k **do**
      Sample mini-batches from the experience replay
      Optimize sum-squared error between its own Q-network and target networks

a random action with probability with ϵ. Following the environment transition because of actions taken all agents, each agent collects and stores the transition tuple, (O_t, O_{t+1}, A_t, R_t), in a experience replay. A mini-batch of experience is uniformly sampled from the memory for updating Q-network and then minimize the sum squared error:

$$\sum_E [R_{t+1} + \gamma maxQ(O_t^k(S_{t+1}, a, \theta^-)) - Q(O_t^k(S_t, A_t, \theta)]^2, \tag{4.5}$$

where θ^- is the parameter set of a target Q-network, which are duplicated from the training Q-network.

4.5.5 Comparison with rule-based solution

Through this subsection, we investigate the need for RL by comparing with rule-based solution. RL generally requires high computation performance. If it works well with

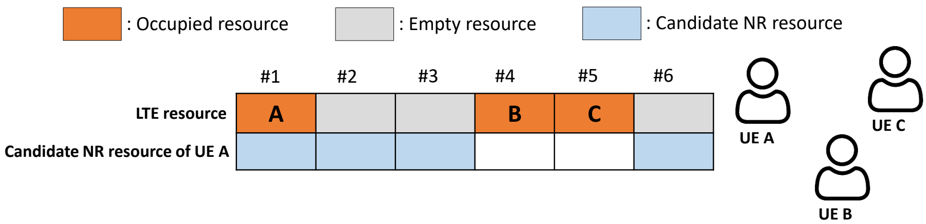

Figure 4.6: Example of rule-based solution.

general rule-based techniques, it is effective in terms of computing performance not to use RL. Therefore, it is important to verify that this problem requires RL.

We assume a ideal rule-based solution that all UEs can learn neighbors' LTE resource selection. Hence, the UEs in the rule-based solution avoid NR resource selection, which cause IDC problem. For example, as shown in Fig. 4.6, there are three UEs, A, B, and C. When UE A selects its NR resource, UE A avoid resources of UEs B and C. Hence, UE A selects its NR resource among resource 1, 2, 3, and 6.

As shown in Fig. 4.7, we confirm that MARL is very close to the ideal result. We also observe that MARL is closer to the ideal performance than the ideal rule-based solution. Thus, we conclude that RL has an excellent effect on solving the IDC problem.

4.6 Performance evaluation

As shown in Fig. 4.8, the larger the guardband size, the better the PDR performance. In case of IDC-free performance, its performance shows an ideal case, which does not have IDC interference. We observe that Multi-Agent Reinforcement Learning (MARL) achieves almost the same NR PDR performance as the IDC-free case. Also, we confirm that MARL achieves almost the same LTE sidelink performance as the guardband at 10 MHz despite simply selecting NR resources.

Among IDC damages, TX-RX cases generally cause the greatest damage. There-

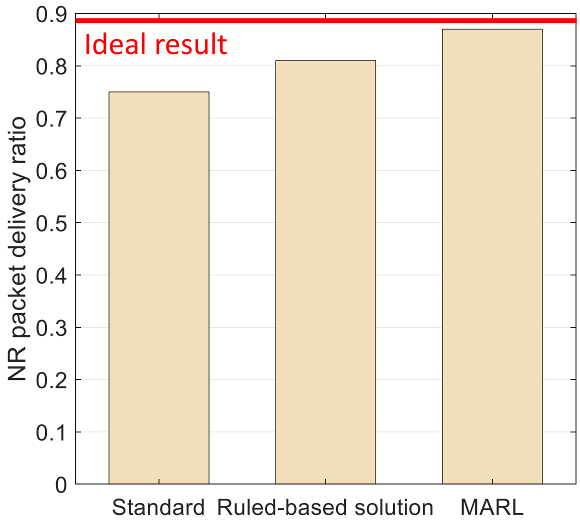

Figure 4.7: Comparison result with rule-based solution.

fore, we design our reward policy to select NR resources by avoiding to cause TX-RX case. As shown in Fig. 4.9, MARL reduces the number of TX-RX occurrences by 15 %. In case of MARL, the number of times that TX-RX occurrences does not occur is twice that of the baseline. That is, our reward policy is designed to avoid the TX-RX occurrences well.

We also observe the PDR performances varying R, the ratio of the number of UEs to the total number of time resources. Fig. 4.10 shows the PDR performance. When R is small, performance improvements cannot be observed because there is little room for resource selection. However, it can be seen that as R gradually increases, the performance gain increases.

4.7 Summary

Through this work, we propose a NR sidelink resource allocation scheme based on multi-agent reinforcement learning, which awares a IDC problem between LTE and NR in Intelligent Transport System (ITS) band. First, we model a realistic IDC inter-

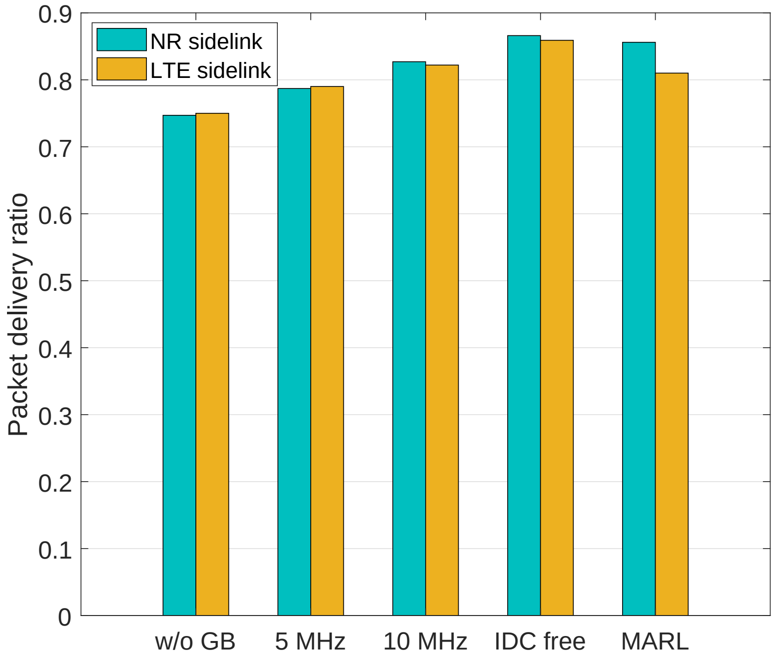

Figure 4.8: PDR performances varying guard band size.

ference based on spectrum emission mask specified at the standard. Then, we formulate the resource allocation as a multi-agent reinforcement learning with fingerprint method. Each UE achieves its local observation and rewards, and learns its policy to increase its rewards through updating Q-network. Through simulation results, we observe that the proposed resource allocation scheme further improves Packet Delivery Ratio (PDR) performances compared to the legacy scheme.

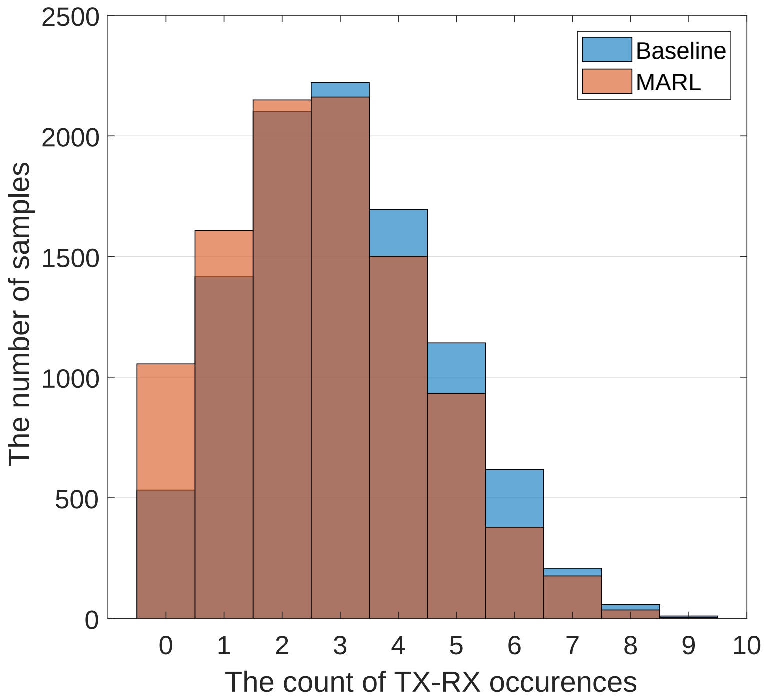

Figure 4.9: Histogram of TX-RX occurrences.

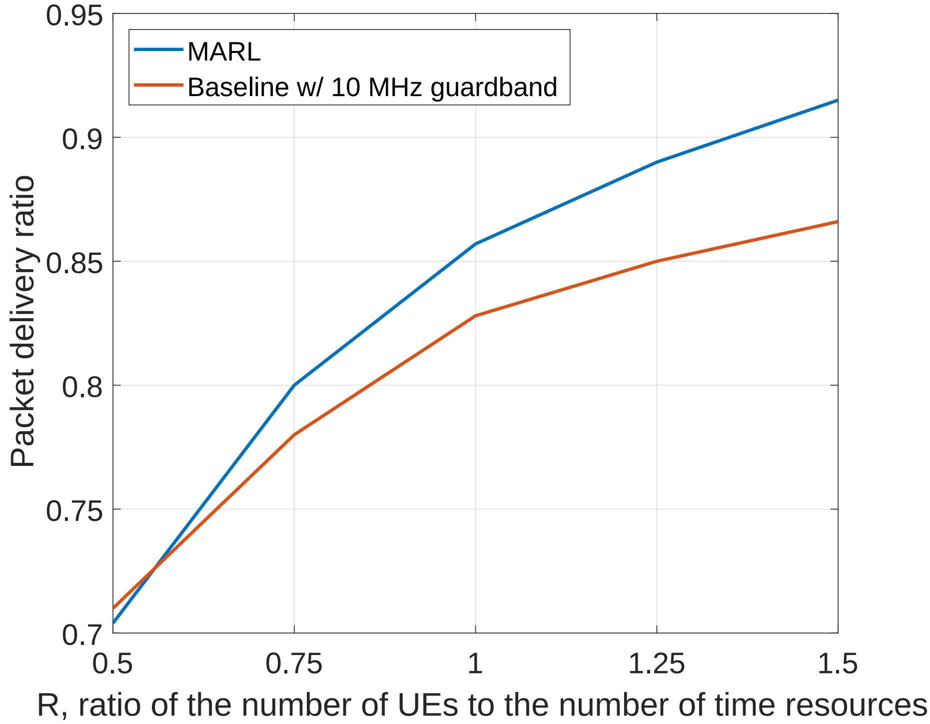

Figure 4.10: PDR performances varying ratio of the number of UEs to the total number of time resources.

Chapter 5

Concluding Remarks

In this dissertation, we have proposed three MAC layer strategies for cellular sidelink performance enhancements.

In Chapter 2, we have presented a feedback mechanism for D2D communication that enable UEs to transmit feedback without the help of BS and the proposed feedback mechanism allows UEs to multiplex on the same RB by using the cyclic shift of Zadoff-Chu sequence. We also propose a groupcast rate adaptation algorithm, FaRRA, that quickly controls MCS level while mitigating in-band emission problem. Through simulation results, we validate that FaRRA outperforms the legacy scheme in terms of goodput.

In Chapter 3, through LTE-V2V communication, UEs transmit Cooperative Awareness Message (CAM), which is a periodic message, and Decentralized Environmental Notification Message (DENM), which is a event-driven message and allows one-hop relay. Thus, we have proposed *CoCo*, which is a context-aware congestion control scheme. *CoCo* consists of two algorithms for each safety messages, i.e., CAM and DENM. Through the proposed congestion control schemes, UEs decide whether to transmit according to their situation. Through simulation results, we show that our proposed schemes outperform comparison schemes as well as the legacy scheme.

In Chapter 4, we propose a NR sidelink resource allocation scheme based on multi-agent reinforcement learning, which awares a IDC problem between LTE and NR in Intelligent Transport System (ITS) band. First, we model a realistic IDC interference based on spectrum emission mask specified at the standard. Then, we formulate the resource allocation as a multi-agent reinforcement learning with fingerprint method. Each UE achieves its local observation and rewards, and learns its policy to increase its rewards through updating Q-network. Through simulation results, we observe that the proposed resource allocation scheme further improves Packet Delivery Ratio (PDR) performances compared to the legacy scheme.

Bibliography

[1] J. Du *et al.*, “A compressed HARQ feedback for D2D multicast communications,” in *Proc. IEEE VTC*, 2012, pp. 1–5.

[2] F. Shi, W. Xu, H. Shen, and C. Zhao, “Coordinated adaptive control in D2D communications based on delayed limited feedback,” in *Proc. IEEE VTC*, 2014, pp. 1–6.

[3] C. Yin, Y. Wang, W. Lin, and X. Wang, “Energy-efficient channel reusing for device-to-device communications underlying cellular networks,” in *Proc. IEEE VTC*, 2014, pp. 1–5.

[4] L. Cottatellucci, “D2D CSI feedback for D2D aided massive MIMO communications,” in *Proc. IEEE SAM*, 2014, pp. 1–5.

[5] I. AlQerm and B. Shihada, “A cooperative online learning scheme for resource allocation in 5G systems,” in *Proc. IEEE ICC*, 2016, pp. 1–7.

[6] M. Botsov, S. Stańczak, and P. Fertl, “Comparison of location-based and CSI-based resource allocation in D2D-enabled cellular networks,” in *Proc. IEEE ICC*, 2015, pp. 1–7.

[7] D. Feng *et al.*, “User selection based on limited feedback in device-to-device communications,” in *Proc. IEEE PIMRC*, 2013, pp. 2851–2855.

[8] J. Park and R. W. Heath, "Multiple-antenna transmission with limited feedback in D2D networks," *IEEE Wireless Communications Letters*, vol. 5, no. 2, pp. 200–203, Apr. 2016.

[9] T. Zhou, B. Xu, T. Xu, H. Hu, and L. Xiong, "User specific link adaptation scheme for D2D network coding multicast," *IET Communications*, vol. 9, no. 3, pp. 367–374, Feb. 2015.

[10] M. Sepulcre, J. Mittag, P. Santi, H. Hartenstein, and J. Gozalvez, "Congestion and awareness control in cooperative vehicular systems," *Proceedings of the IEEE*, vol. 99, no. 7, pp. 1260–1279, 2011.

[11] A. Vesco, R. Scopigno, C. Casetti, and C.-F. Chiasserini, "Investigating the effectiveness of decentralized congestion control in vehicular networks," in *2013 IEEE Globecom Workshops (GC Wkshps)*. IEEE, 2013, pp. 1314–1319.

[12] A. Rostami, B. Cheng, G. Bansal, K. Sjöberg, M. Gruteser, and J. B. Kenney, "Stability challenges and enhancements for vehicular channel congestion control approaches," *IEEE Transactions on Intelligent Transportation Systems*, vol. 17, no. 10, pp. 2935–2948, 2016.

[13] C. B. Math, H. Li, S. H. de Groot, and I. G. Niemegeers, "V2x application-reliability analysis of data-rate and message-rate congestion control algorithms," *IEEE Communications Letters*, vol. 21, no. 6, pp. 1285–1288, 2017.

[14] S. Subramanian, M. Werner, S. Liu, J. Jose, R. Lupoaie, and X. Wu, "Congestion control for vehicular safety: synchronous and asynchronous mac algorithms," in *Proceedings of the ninth ACM international workshop on Vehicular inter-networking, systems, and applications*, 2012, pp. 63–72.

[15] A. Autolitano, C. Campolo, A. Molinaro, R. M. Scopigno, and A. Vesco, "An insight into decentralized congestion control techniques for vanets from etsi ts 102 687 v1. 1.1," in *2013 IFIP Wireless Days (WD)*. IEEE, 2013, pp. 1–6.

[16] Y. P. Fallah, C. Huang, R. Sengupta, and H. Krishnan, “Congestion control based on channel occupancy in vehicular broadcast networks,” in *2010 IEEE 72nd Vehicular Technology Conference-Fall*. IEEE, 2010, pp. 1–5.

[17] X. Shen, X. Cheng, R. Zhang, B. Jiao, and Y. Yang, “Distributed congestion control approaches for the ieee 802.11 p vehicular networks,” *IEEE intelligent transportation systems magazine*, vol. 5, no. 4, pp. 50–61, 2013.

[18] L. Le, R. Baldessari, P. Salvador, A. Festag, and W. Zhang, “Performance evaluation of beacon congestion control algorithms for vanets,” in *2011 IEEE Global Telecommunications Conference-GLOBECOM 2011*. IEEE, 2011, pp. 1–6.

[19] H.-J. Günther, R. Riebl, L. Wolf, and C. Facchi, “Collective perception and decentralized congestion control in vehicular ad-hoc networks,” in *2016 IEEE Vehicular Networking Conference (VNC)*. IEEE, 2016, pp. 1–8.

[20] G. Bansal, J. B. Kenney, and C. E. Rohrs, “Limeric: A linear adaptive message rate algorithm for dsrc congestion control,” *IEEE Transactions on Vehicular Technology*, vol. 62, no. 9, pp. 4182–4197, 2013.

[21] M. Sepulcre, J. Gozalvez, J. Harri, and H. Hartenstein, “Contextual communications congestion control for cooperative vehicular networks,” *IEEE Transactions on Wireless Communications*, vol. 10, no. 2, pp. 385–389, 2010.

[22] G. Bansal, H. Lu, J. B. Kenney, and C. Poellabauer, “Embarc: Error model based adaptive rate control for vehicle-to-vehicle communications,” in *Proceeding of the tenth ACM international workshop on Vehicular inter-networking, systems, and applications*, 2013, pp. 41–50.

[23] L. Zhang and S. Valaee, “Congestion control for vehicular networks with safety-awareness,” *IEEE/ACM Transactions on Networking*, vol. 24, no. 6, pp. 3290–3299, 2016.

[24] Z. Hu, R. Susitaival, Z. Chen, I.-K. Fu, P. Dayal, and S. K. Baghel, "Interference avoidance for in-device coexistence in 3gpp lte-advanced: Challenges and solutions," *IEEE Communications Magazine*, vol. 50, no. 11, pp. 60–67, 2012.

[25] W. Wang, Y. Lu, H. Xu, and H. Zhou, "In-device coexistence interference evaluation and detection in lte-a system," in *2012 IEEE 75th Vehicular Technology Conference (VTC Spring)*. IEEE, 2012, pp. 1–5.

[26] M. F. Marzban, M. Ismail, M. M. Abdallah, M. M. Khairy, K. Qaraqe, and E. Serpedin, "Idc interference-aware resource allocation for lte/wlan heterogeneous networks," *IEEE Wireless Communications Letters*, vol. 4, no. 6, pp. 581–584, 2015.

[27] S. K. Baghel, M. A. Ingale, and G. Goyal, "Coexistence possibilities of lte with ism technologies and gnss," in *2011 National Conference on Communications (NCC)*. IEEE, 2011, pp. 1–5.

[28] L. Liang, H. Ye, and G. Y. Li, "Spectrum sharing in vehicular networks based on multi-agent reinforcement learning," *IEEE Journal on Selected Areas in Communications*, vol. 37, no. 10, pp. 2282–2292, 2019.

[29] H. Ye, G. Y. Li, and B.-H. F. Juang, "Deep reinforcement learning based resource allocation for v2v communications," *IEEE Transactions on Vehicular Technology*, vol. 68, no. 4, pp. 3163–3173, 2019.

[30] H. Yang, X. Xie, and M. Kadoch, "Intelligent resource management based on reinforcement learning for ultra-reliable and low-latency iov communication networks," *IEEE Transactions on Vehicular Technology*, vol. 68, no. 5, pp. 4157–4169, 2019.

[31] Simulation of urban mobility. [Online]. Available: http://sumo.dlr.de

[32] "Cisco visual networking index: Global mobile data traffic forecast update, 2015-2020," Feb. 2016. [Online]. Available: http://www.cisco.com/go/vni

[33] 3GPP TS 23.303, "Proximity-based services (ProSe); stage 2," ver. 12.0.0, Mar. 2015.

[34] J.-M. Vella and S. Zammit, "A survey of multicasting over wireless access networks," *IEEE Communications Surveys & Tutorials*, vol. 15, no. 2, pp. 718–753, 2013.

[35] G. Araniti *et al.*, "A solution to the multicast subgroup formation problem in LTE system," *IEEE Wireless Communications Letters*, vol. 4, no. 2, pp. 149–152, Apr. 2015.

[36] V. Gupta *et al.*, "Experimental evaluation of large scale WiFi multicast rate control," in *Proc. IEEE INFOCOM*, 2016, pp. 1–9.

[37] M. Du, X. Wang, D. Wang, and Y. Wang, "Device-to-device dynamic clustering algorithm in multicast communication," in *Dependable, Autonomic and Secure Computing (DASC), 2013 IEEE 11th International Conference on*. IEEE, 2013, pp. 578–582.

[38] K. Chi, L. Huang, Y. Li, Y.-h. Zhu, X.-z. Tian, and M. Xia, "Efficient and reliable multicast using device-to-device communication and network coding for a 5g network," *IEEE Network*, vol. 31, no. 4, pp. 78–84, 2017.

[39] B. W. Khoueiry and M. R. Soleymani, "A novel coding strategy for device-to-device communications," in *Consumer Communications and Networking Conference (CCNC), 2015 12th Annual IEEE*. IEEE, 2015, pp. 200–205.

[40] B. Zhou, H. Hu, S.-Q. Huang, and H.-H. Chen, "Intracluster device-to-device relay algorithm with optimal resource utilization," *IEEE Transactions on Vehicular Technology*, vol. 62, no. 5, pp. 2315–2326, 2013.

[41] Q. Hu and J. Zheng, "An efficient network coding based multicast retransmission scheme for mobile communication networks with relays," in *Communications (ICC), 2012 IEEE International Conference on*. IEEE, 2012, pp. 5413–5417.

[42] S. Wang, C. Gong, X. Wang, and M. Liang, "An efficient retransmission strategy for wireless scalable video multicast," *IEEE Wireless Communications Letters*, vol. 1, no. 6, pp. 581–584, 2012.

[43] C. Zhan, Y. Xu, J. Wang, and V. Lee, "Reliable multicast in wireless networks using network coding," in *Mobile Adhoc and Sensor Systems, 2009. MASS'09. IEEE 6th International Conference on*. IEEE, 2009, pp. 506–515.

[44] P. Fan, C. Zhi, C. Wei, and K. B. Letaief, "Reliable relay assisted wireless multicast using network coding," *IEEE Journal on Selected Areas in Communications*, vol. 27, no. 5, 2009.

[45] H. Wu and J. Zheng, "Network coding based multicast retransmission for mobile communication networks," in *Communication Technology (ICCT), 2010 12th IEEE International Conference on*. IEEE, 2010, pp. 235–238.

[46] X. Zhang, M. Yang, L. Wang, and M. Sun, "An openflow-enabled elastic loss recovery solution for reliable multicast," *IEEE Systems Journal*, 2016.

[47] H. Lee and D.-H. Cho, "Control overhead reduction based on dedicated retransmission scheme in reliable multicast services," *IEEE Communications Letters*, vol. 11, no. 9, 2007.

[48] 3GPP TR 36.843, "Study on LTE device to device proximity services; radio aspects," ver. 12.0.1, Mar. 2014.

[49] WINNER+ Deliverables, "WINNER+ final channel models," D5.3, June 2010.

[50] Draft new Report ITU-R M.[IMT.EVAL], "Guidelines for evaluation of radio interface technologies for IMT-advanced," Nov. 2008.

[51] WHO, Road traffic injuries. [Online]. Available: https://www.who.int/news-room/fact-sheets/detail/road-traffic-injuries

[52] 3GPP TS 36.213, "Technical specification group radio access network; evolved universal terrestrial radio access (E-UTRA); physical layer procedures," ver. 15.5.0, Mar. 2019.

[53] Qualcomm, Accelerating C-V2X commercialization. [Online]. Available: https://www.qualcomm.com/documents/path-5g-cellular-vehicle-everything-c-v2x

[54] 5GAA White paper, "White Paper on ITS spectrum utilization in the Asia Pacific Region," July 2018.

[55] ——, "An assessment of LTE-V2X (PC5) and 802.11p direct communications technologies for improved road safety in the EU," Dec. 2017.

[56] ETSI TS 302 637-2, "Intelligent Transport Systems (ITS); Vehicular Communications; Basic Set of Applications; Part 2: Specification of Cooperative Awareness Basic Service," V1.3.2, Nov. 2011.

[57] ETSI TS 302 637-3, "Intelligent Transport Systems (ITS); Vehicular Communications; Basic Set of Applications; Part 3: Specification of Decentralized Environmental Notification Basic Service," V1.3.2, Nov. 2014.

[58] 3GPP TR 36.885, "Technical Specification Group Radio Access Network; Study on LTE-based V2X Services," ver. 14.0.0, June 2016.

[59] D. Jiang, Q. Chen, and L. Delgrossi, "Optimal data rate selection for vehicle safety communications," in *Proc. ACM VANET*, 2008, pp. 30–38.

[60] ETSI TR 101 612, "Intelligent Transport Systems (ITS); Cross Layer DCC Management Entity for Operation in the ITS G5A and ITS G5B Medium; Report on Cross Layer DCC Algorithms and Performance Evaluation," V1.1.1, Sept. 2014.

[61] F. J. Martinez *et al.*, “A street broadcast reduction scheme (”sbr”) to mitigate the broadcast storm problem in vanets,” *Wireless personal Commun.*, vol. 56, no. 3, pp. 559–572, 2011.

[62] G. Korkmaz, E. Ekici, and F. Ozguner, “An efficient fully ad-hoc multi-hop broadcast protocol for inter-vehicular communication systems,” in *Proc. IEEE ICC*, vol. 1, June 2006, pp. 423–428.

[63] D. Li *et al.*, “A distance-based directional broadcast protocol for urban vehicular ad hoc network,” in *Proc. IEEE WiCom*, 2007, pp. 1520–1523.

[64] Y.-C. Tseng, S.-Y. Ni, Y.-S. Chen, and J.-P. Sheu, “The broadcast storm problem in a mobile ad hoc network,” *Wireless Netw.*, vol. 8, no. 2-3, pp. 153–167, 2002.

[65] N. Wisitpongphan *et al.*, “Broadcast storm mitigation techniques in vehicular ad hoc networks,” *IEEE Wireless Commun.*, vol. 14, no. 6, pp. 84–94, 2007.

[66] A. Wegener *et al.*, “AutoCast: An adaptive data dissemination protocol for traffic information systems,” in *Proc. IEEE VTC*, 2007, pp. 1947–1951.

[67] Q. Xiang *et al.*, “Data preference matters: A new perspective of safety data dissemination in vehicular ad hoc networks,” in *Proc. IEEE INFOCOM*, Apr. 2015, pp. 1149–1157.

[68] S. Busanelli, G. Ferrari, and R. Gruppini, “Performance analysis of broadcast protocols in vanets with poisson vehicle distribution,” in *2011 11th International Conference on ITS Telecommunications*. IEEE, 2011, pp. 133–138.

[69] T. Bai and R. W. Heath, “Coverage and rate analysis for millimeter-wave cellular networks,” *IEEE Transactions on Wireless Communications*, vol. 14, no. 2, pp. 1100–1114, 2014.

[70] J. G. Andrews, F. Baccelli, and R. K. Ganti, “A tractable approach to coverage and rate in cellular networks,” *IEEE Transactions on communications*, vol. 59, no. 11, pp. 3122–3134, 2011.

[71] 3GPP TR 36.885, “Technical Specification Group Radio Access Network; Study on LTE-based V2X Services,” V2.0.0, June 2016.

[72] M. Rupp, S. Schwarz, and M. Taranetz, *The Vienna LTE-Advanced Simulators: Up and Downlink, Link and System Level Simulation*, 1st ed., ser. Signals and Communication Technology. Springer Singapore, 2016.

[73] The network simulator-3. [Online]. Available: https://www.nsnam.org/

[74] 3GPP TS 36.101, “UE radio transmission and reception,” ver. 15.1.0, Jan. 2018.

[75] J. Foerster, N. Nardelli, G. Farquhar, T. Afouras, P. H. Torr, P. Kohli, and S. Whiteson, “Stabilising experience replay for deep multi-agent reinforcement learning,” in *Proceedings of the 34th International Conference on Machine Learning-Volume 70*. JMLR. org, 2017, pp. 1146–1155.

초 록

전형적인 셀룰러 통신에서는, 단말들은 서로 통신하기 위해 항상 기지국을 거쳐야 한다. 예를 들면, 단말이 uplink를 통해 기지국에게 패킷을 전송한 다음 기지국은 downlink를 통해 해당 패킷을 전송해준다. 이러한 통신방식은 단말들에게 효율적으로 서비스를 제공할 수 있지만, 상황에 따라서는 지연문제와 기지국의 과부하 문제를 야기할 수 있다. 따라서 3GPP release12에서 이러한 문제점들을 극복하기 위해 sidelink가 제안되었다. 덕분에 단말들은 sidelink를 통해서 서로 직접 통신을 할 수 있게 되었다.

Sidelink를 사용하는 두 가지 대표적인 통신은 D2D(Device-to-Device) 통신과 V2V(Vehicle-to-Vehicle) 통신이다. 본 논문에서는 D2D 와 V2V 통신 성능을 향상시키기 위한 세가지 전략을 고려한다. (i) D2D 통신을 위한 효율적인 피드백 메커니즘, (ii) V2V 통신을 위한 상황인식기반 혼잡제어 기법, 그리고 (iii) IDC(In-Device Coexistence) 인지 기반 sidelink 자원 할당 방식.

첫째, 관련 표준에는 D2D 통신이 브로드캐스트 유형의 통신만을 지원하기 때문에 D2D 통신에 대한 피드백 메커니즘이 없다. 우리는 이러한 한계점을 극복하고자 D2D 통신을 위한 피드백 메커니즘을 제안한다. 제안된 메커니즘을 통해, 단말은 기지국의 도움없이 피드백 메커니즘을 사용할 수 있으며 피드백 자원을 할당하기 위한 추가 신호를 필요로 하지 않는다. 우리는 또한 제안된 피드백 메커니즘위에서 동작할 수 있는 data rate 조절 기법을 제안하였다. 우리는 시뮬레이션 결과를 통하여, 제안한 data rate 조절 기법이 기존 방식보다 더 높고 안정적인 수율을 제공하는 것을 확인하였다.

둘째, LTE-V2V 통신을 위한 상황 인지 기반 혼잡 제어 기법을 제안한다. LTE-V2V 통신에서 단말들은 주기적인 메시지인 CAM(Cooperative Awareness Message) 및 비주기적 메시지이며 one-hop릴레이를 허용하는 DENM(Decentralized Environmental Notification Message)를 전송한다. 위의 두 메시지는 특성과 생성 규칙이 다르기 때문에 동일한 혼잡 제어 기법을 적용하는 것은 비효율적이다. 따라서 우리는 각 메시지에 적용할 수 있는 혼잡 제어 기법들을 제안한다. 제안된 기법들을 통해서 단말들은 그들의 상황에 따라서 전송 여부를 결정하게 된다. 시뮬레이션 결과를 통해 제안된 기법이 기존 표준 방식 뿐만 아니라 최신의 비교 기법들보다 우수한 성능을 얻는 것을 확인하였다.

마지막으로 ITS(Intelligent Transport System)대역에서 LTE와 NR사이의 IDC문제를 고려하는 NR sidelink 자원할당 기법을 제안한다. 먼저, 표준에 지정된 스펙트럼 방출 마스크를 기반으로 현실적인 IDC 간섭을 모델링한다. 그런 다음 다중 에이전트 강화학습으로 자원할당 기법을 제안한다. 각 단말들은 자신들의 주변 환경을 관측하고 관측된 환경을 기반으로 행동하여 보상을 얻고 Q-network을 자신의 보상을 증가시키도록 정책을 업데이트 및 학습한다. 우리는 시뮬레이션 결과를 통하여 제안된 자원할당 박식이 기존기법 대비하여 PDR(Packet Delivery Ratio) 성능을 향상시키는 것을 확인하였다.

주요어: LTE, NR, 단말 간 직접 통신, 차량 간 직접 통신, 피드백 메커니즘, 혼잡 제어 기법, 단말 내 공존 문제, 강화 학습.

학번: 2014-21660

감사의 글

대학원을 입학한 뒤 6년 반이라는 시간이 지난 뒤 이제는 졸업을 앞 둔 시점에서 저는 여러가지 감정들이 교차합니다. 한마디로 표현하자면 흔하디 흔한 표현이지만 시원하면서 섭섭합니다. 학위과정 동안 고민했던 연구들을 마무리 지었다는 홀가분함과 동시에 다른 방식으로 했다면 더 나은 결과물을 낼 수 있지 않았을까 등 여러가지 사안에 대해 양가적 감정이 드는 것 같습니다. 그래서 제가 느끼는 여러 감정들을 전부 서술하게 된다면 결국에는 아무 결론없는 글이 될 것이기에 제가 느끼는 감정 중 양가적이지 않은 감정에 대하여 서술하고자 그 부분을 고민해보았습니다. 고민의 결과 제 주변 사람들에게 감사한 마음 만큼은 오롯이 감사한 마음뿐이라고 느꼈습니다. 그래서 저는 이 페이지를 빌어서 제 주변 분들에 대한 감사함을 표하고자 합니다.

제게 훌륭한 배움의 기회를 주신 은사님들에게 먼저 감사함을 말씀드리고 싶습니다. 매 주 주말마다 논문학습지도를 해주신 이병기 교수님 정말 감사드립니다. 덕분에 다양한 논문들을 읽을 기회를 갖게 되었고 논문이 어떤식으로 형성되는지 그리고 논문을 어떻게 읽어야 하는지에 대하여 수련하고 공부할 수 있었습니다. 현재는 삼성리서치에서 근무하시는 최성현 전 교수님에게도 열정적인 연구지도에 대하여 감사드립니다. 교수님과의 수많은 연구미팅을 통하여 연구를 어떻게 접근해야하는지 그리고 어떻게 연구를 해야 하는지에 대하여 정말 많은 가르침을 받았습니다. 또한 교수님의 어떠한 상황에서도 늘 발전하고자 하는 자세는 저에게 많은 귀감이 되었습니다.

그리고 학생들에게 늘 진심과 온정으로 지도해주시는 박세웅 교수님께도 진심으로 감사드립니다. 교수님께서 해주시는 말씀들은 제가 앞으로 어떤 사람이 되어야

겠다 라는 방향을 갖게 해주셨습니다. 앞으로도 교수님의 말씀 가슴속에 잘 새기고 살아가도록 하겠습니다. 또한 제 학위 심사를 위하여 귀중한 시간을 내어주신 심병효 교수님, 이경한 교수님, 오정석 교수님, 백정엽 교수님께도 무한한 감사를 드립니다. 교수님들 덕분에 더 나은 학위논문을 완성할 수 있었습니다. 6년 반이라는 시간 동안 훌륭하신 세분의 은사님을 비롯하여 네분의 교수님들을 만나뵙고 지도를 받을 수 있었던것은 제게 정말 큰 행운이었습니다. 앞으로 살아가며 제가 은사님들에게 받은 가르침들을 배풀며 살아가도록 하겠습니다. 감사합니다.

다음으로는 제 선후배님들과 동기들에게 감사함을 표하고자 합니다. 선후배님들과 동기들은 6년 반이라는 시간 동안 연구뿐만아니라 심적으로도 직접적으로 큰 의지가 되었던 분들이라고 생각합니다. 선후배님들과 동기들의 도움이 없었다면 저는 지금 이 시기에 졸업을 하지 못했을 것이라고 생각합니다. 제가 처음 연구실 생활을 시작하였을 때 연구실 생활에 적응하고 재미를 느끼고 해준 연구실 방장 연철이형에게 특별히 감사함을 전하고 싶습니다. 또한 연구실에서 제가 소속된 첫 팀의 팀장이셨던 종우형에게도 특별히 감사함을 전하고 싶습니다.

그리고 곧 졸업을 앞둔 기택이와 철영이에게도 오랜시간 동안 후배로서, 동료로서 그리고 친구로서 저에게 많은 도움을 주었기에 감사함을 표하고 원하는 바를 다 이루고 졸업하길 바랍니다. 마찬가지로 지환이와 선욱이에게도 감사함을 표 하고 원하는 바를 다 이루길 바랍니다. 일일이 수많은 선후배님들을 거론하며 제 감사함을 표하기에는 하나의 챕터를 할애하더라도 부족할 것 같습니다. 혹여 거론되지 않으셨더라도 제가 가지고 있는 감사하는 마음은 차이가 결코 없음을 말씀드리고 싶습니다. 넓은 아량으로 이해해주시면 감사하겠습니다. 선후배님들이 있었기에 저는 무사히 졸업을 할 수 있었습니다. 다시 한번 진심으로 감사드리고 늘 행복이 가득하길 기원합니다.

제 동기 준석이형, 지훈이, 재홍이 그리고 졸업한 순원이에게도 정말로 고맙고 감사하다고 전하고 싶습니다. 힘들때나 즐거울때나 동기들과 함께 할 수 있어서 정말 행운이었습니다. 앞으로도 제 동기들 원하는바 다 이루고 지금과 같이 서로 힘이 될 수 있으면 좋겠습니다. 그리고 한 학기씩 차이 나지만 동기처럼 지낸 영욱이와 준영이에게도 감사의 인사를 전하고 싶습니다. 여러분과 함께 지내온 연구실 생활

들은 늘 가슴 한편에 좋은 추억으로 남아있을 것 같습니다.

그리고 함께 연구실 생활을 하지는 않았지만 대학친구 중 같은 길을 걸어가고 있는 기영이와 현재에게도 진심의 감사를 표하고 싶습니다. 뛰어난 능력으로 마지막까지 잘 마무리하여 원하는 바를 꼭 이루고 졸업하길 바랍니다. 그리고 마음의 위안과 격려를 준 친구 유원이에게도 감사함을 표하고자 합니다. 곧 꾸리게 될 가정에도 늘 행운과 행복이 가득하길 바랍니다.

묵묵히 저를 믿고 지지해주시는 아버지 그리고 헌신으로 저를 양육해주신 어머니께 깊은 사랑과 감사를 전하고 싶습니다. 또한 고집스럽고 때로는 미성숙한 저를 사랑으로 보듬어 주셔서 감사합니다. 두 분의 존재는 제게 늘 그늘을 주는 버팀목과 같았습니다. 무뚝뚝한 자식이라 표현하지 못하였지만 두 분 존경하고 사랑합니다. 마지막으로 여자친구 예승이에게 감사의 마음을 표현하고 싶습니다. 8년 넘게 제 옆에서 힘들 때나 슬플 때나 함께 해주었음에 감사함과 존경을 표현하고 싶습니다. 한결같이 내옆에 있어줘서 정말 고맙고 사랑합니다.

이 외에도 저는 많은 분들의 도움을 받았습니다. 그분들을 일일이 찾아뵙고 감사함을 표하는 것은 현실적으로 어려울 것이라는 생각이 듭니다. 대신 저는 그분들에게 받은 도움을 기억하며 저 또한 다른 사람들에게 배풀며 살아가면서 감사함을 보답하겠습니다.

감사합니다.

2020 년 8월

윤호영 올림